Aalto University
School of Electrical
Engineering

Turo Halinen

DISTRIBUTED TRANSMISSION FOR COOPERATIVE WIRELESS NETWORKS

Thesis submitted for examination for the degree of Licentiate of Science in Technology, Espoo, 9 April, 2013.

Supervisor: Professor Jyri Hämäläinen

Instructor: D.Sc. (Tech) Alexis A. Dowhuszko

Aalto University

AALTO UNIVERSITY SCHOOLS OF TECHNOLOGY PO Box 11000, FI-00076 AALTO http://www.aalto.fi	ABSTRACT OF THE LICENTIATE THESIS

Author:	Turo Halinen		
Title:	DISTRIBUTED TRANSMISSION FOR COOPERATIVE WIRELESS NETWORKS		
School:	School of Electrical Engineering	Department:	Department of Communications and Networking
Research field:	Telecommunications	Code:	S016Z
Supervisor:	Jyri Hämäläinen	Instructor(s):	Alexis A. Dowhuszko
Examiner(s):	Stefan Werner		

Abstract:

In this thesis the impact of quantized channel feedback on the performance of a (coherent) distributed beamforming (DBF) scheme is studied. The analysis is done in the context of a wireless access network, and the goal is to provide an adequate broadband coverage for users located inside buildings. In the examined scenario, instead of trying to reach the serving base station (BS) directly, it is assumed that each mobile station (MS) receives assistance from a cooperative group of network elements that is placed in close proximity (e.g., in the same room or office). This cluster of cooperative network elements is formed by a large number of low-cost low-power relaying stations (RSs), which have fixed locations and are equipped with only one antenna.

Closed-form approximations for three different performance measures are derived (i.e., outage capacity, ergodic capacity, and bit error probability), providing performance predictions and fundamental limits of the proposed system architecture. The analysis reveals that the end-to-end performance that is achieved when using a small amount of phase feedback information (per RS in the second hop) is very close to the full phase information upper bound, paving the way to use massive DBF architectures as a practical way to cope with high data rate in future wireless systems.

In addition, to give grounds for the suggested DBF scheme, fundamental information on cooperative communication is given first. Concepts of relaying, heterogeneous networks, and multi antenna techniques are given a brief introduction in this thesis.

Date: 9.4.2013	Language: English	Number of pages: 102

Keywords: Cooperative communications, distributed beamforming, decode-and-forward relays, heterogeneous networks, limited feedback information, massive network element deployments, non-perfect channel knowledge, performance prediction.

Aalto-yliopisto

AALTO-YLIOPISTO TEKNIIKAN KORKEAKOULUT PL 11000, 00076 AALTO http://www.aalto.fi	LISENSIAATINTUTKIMUKSEN TIIVISTELMÄ

Tekijä: Turo Halinen

Työn nimi: HAJAUTETUN KEILANMUODOSTUKSEN SUORITUSKYKYANALYYSI YHTEISTOIMINNALLISILLE LANGATTOMILLE VERKOILLE

Korkeakoulu: Sähkötekniikan korkeakoulu	Laitos: Tietoliikenne- ja tietoverkkotekniikan laitos
Tutkimusala: Tietoliikennetekniikka	Koodi: S016Z
Työn vastuuprofessori: Jyri Hämäläinen	Työn ohjaaja(t): Alexis A. Dowhuszko

Työn ulkopuolinen tarkastaja(t): Stefan Werner

Tiivistelmä:

Tässä työssä tutkitaan kvantisoidun takaisinkytkentäkanavan vaikutusta hajautetun keilanmuodostuksen (DBF) suorituskykyyn. Analyysin systeemimalli olettaa langattoman liityntäverkon missä tavoitteena on tarjota riittävä laajakaistapeitto käyttäjille rakennusten sisätiloissa. Tutkitussa skenaariossa, sen sijaan, että yritettäisiin saada suora yhteys palvelevaan tukiasemaan (BS), oletetaan, että jokainen käyttäjälaite (MS) saa tukea yhteistoiminnalliselta ryhmältä verkkoelementtejä, jotka on sijoitettu MS:n läheisyyteen (esim. samaan huoneeseen tai toimistoon). Tämä joukko verkkoelementtejä koostuu suuresta määrästä edullisia pienitehoisia toistinasemia (RS), joilla on kiinteä sijainti.

Suljetun muodon tuloksia johdetaan kolmelle eri suorituskyvyn mittarille (eli outage-kapasiteetti, ergodinen kapasiteetti, ja bittivirhetodennäköisyys), tarjoten suorituskyvyn ennusteita ja perustavaa laatua olevia suorituskykyrajoja ehdotettuun järjestelmään. Analyysi paljastaa, että suorituskyky, joka saavutetaan käyttämällä pientä määrää vaihepalautetta (toisessa hypyssä) on hyvin lähellä ylärajaa mikä saavutetaan täydellisellä vaiheinformaatiolla. Tulokset pohjustavat massiivisten DBF-arkkitehtuurien käyttöönottoa käytännön keinona selviytyä suurista datanopeuksista tulevaisuuden langattomissa järjestelmissä.

Suorituskykyanalyysin lisäksi työn alussa on taustan esittelemiseksi annettu pohjatietoja ehdotetulle DBF järjestelmälle sekä yhteistoiminnalliselle viestinnälle yleisellä tasolla. Lisäksi on esitelty toistimien, heterogeenisten verkkojen ja moniantennitekniikoiden käsitteet.

Päivämäärä:	9.4.2013	Kieli:	Englanti	Sivumäärä:	102

Avainsanat: yhteistoiminnallinen viestintä, hajautettu keilanmuodostus, dekoodaava ja edelleen lähettävä toistinasema, moninainen verkko, rajoitettu takaisinkytkentäinformaatio, tiheä verkkoelementtien sijoitus, osittainen kanavatieto, suorituskyvyn ennustaminen.

Preface

This work has been carried out at the department of Communications and Networking of Aalto University during 2010-2012. It has been funded as a part of the IMANET project.
I would like to thank my supervisor Prof. Jyri Hämäläinen, who granted me this great opportunity, and Dr Alexis Dowhuszko, who helped me more than he really needed to.

Helsinki, April 9, 2013,

Turo Halinen

Contents

Preface iv

Contents v

List of Publications vii

Author's Contribution viii

1. Introduction 1

1.1 Motivation 1

1.2 Goals of the Research 3

1.3 Research Justification 3

1.4 Structure of the Thesis 4

2. Fundamentals of Cooperative Communications 5

2.1 Relaying Concepts 6

2.2 Heterogeneous Network Approach 8

2.3 Multi-Antenna Techniques 9

2.3.1 Beamforming 10

2.4 Distributed Antenna Systems 12

2.4.1 Distributed Beamforming 14

3. System Model 17

3.1 Signal Model 18

3.2 Assumptions on System Model 19

3.3 Feedback Approaches 20

4. Performance Analysis 22

4.1 Individual Feedback Channel 22

4.1.1 Central and Non-Central Chi-Square Distributions . 23

4.1.2 PDF and CDF Approximations in Case of Large Number of Array Elements . . . 25
4.2 Performance Analysis of Distributed Beamforming with Limited Feedback . . . 27
4.2.1 Outage Probability . . . 28
4.2.2 Ergodic Capacity . . . 28
4.2.3 Bit Error Probability . . . 30

5. Numerical Results **32**
5.1 Performance of Dedicated Feedback Channel Scheme . . . 32
5.1.1 Outage Probability . . . 33
5.1.2 Ergodic Capacity . . . 36
5.1.3 Bit Error Probability . . . 37

6. Common Feedback Approach **40**
6.1 Differences to the Scheme Presented by Mudumbai . . . 41
6.2 Common Feedback Channel . . . 41
6.2.1 Random Walk . . . 42
6.3 Single Receiver . . . 44
6.4 Multiple Receivers . . . 45

7. Conclusions **48**
7.1 Summary of Conclusions . . . 48
7.2 Future Work . . . 49

Bibliography **52**

Publications **55**

List of Publications

This thesis consists of an overview and of the following publications which are referred to in the text by their Roman numerals.

I Turo Halinen, Alexis A. Dowhuszko, and Jyri Hämäläinen. Performance of Distributed Beamforming for Dense Relay Deployments in Presence of Limited Feedback Information. *Submitted to EURASIP Journal on Advances in Signal Processing Special Issue on "Advanced Distributed Wireless Communication Techniques - Theory and Practice"*, Jun. 2012.

II Alexis A. Dowhuszko, Turo Halinen, Jyri Hämäläinen, and Olav Tirkkonen. Performance of Relay-Aided Distributed Beamforming Techniques in Presence of Limited Feedback Information. In *Conference on Performance, Safety and Robustness in Complex Systems and Applications 2011*, pp. 28-34, Apr. 2011.

Author's Contribution

Publication I: "Performance of Distributed Beamforming for Dense Relay Deployments in Presence of Limited Feedback Information"

The author had a leading role in writing the paper, performing the theoretical modeling, and conducting the new simulations.

Publication II: "Performance of Relay-Aided Distributed Beamforming Techniques in Presence of Limited Feedback Information"

The author participated in the theoretical modeling, simulations and writing of the paper.

List of Abbreviations and Symbols

Abbrevations

3GPP	Third general partnership project
AF	Amplify-and-forward
AP	Access point
AWGN	Additive white Gaussian noise
BEP	Bit error probability
BPSK	Binary phase-shift keying
BPU	Baseband processing unit
BS	Base station
CCI	Co-channel interference
CDF	Cumulative distribution function
CoMP	Coordinated multi-point
CSI	Channel state information
CU	Central unit
DAS	Distributed antenna system
DBF	Distributed beamforming
DF	Decode-and-forward
eNB	Evolved Node B
FBS	Femto base station
FUE	Femto user equipment

HeNB	Home evolved Node B
HetNet	Heterogeneous network
i.i.d.	Independent and identically distributed
LOS	Line-of-sight
LTE	Long term evolution
MBS	Macro base station
MIMO	Multiple-input multiple-output
MMSE	Minimum mean square error
MS	Mobile station
MVDR	Minimum variance distortionless response
NLOS	Non-line-of-sight
PDF	Probability distribution function
QoS	Quality of service
RAU	Remote antenna unit
RF	Radio frequency
RS	Relay station
RV	Random variable
RW	Random walk
SINR	Signal-to-interference-plus-noise power ratio
SNR	Signal-to-noise power ratio
UMTS	Universal mobile telecommunications system

Symbols

$(b)_n$	Pochhammer's symbol/ rising factorial
α, i, k, m, n	indexes
$\bar{p_e}$	average bit error probability
δ	power imbalance between two array element groups
δ_m	random phase pertubation
γ	aggregate SNR
$\Gamma(\bullet)$	Gamma function
γ_0	SNR threshold
γ_m	received SNR from the m-th array element
$\gamma_{ij,m}$	m-th receiver SNR from user i to user j
κ	deterministic-to-random component energy ratio
$\mathcal{F}_Z$	fading figure
$\mathcal{Q}$	quantization set
μ	mean
μ_I	mean of $\widetilde{X}_I$
μ_R	mean of $\widetilde{X}_R$
ν	maximum value of the random walker
$\overline{\gamma}$	average SNR
ϕ_m	m-th phase from the quantization set Q
ψ_m	channel phase response from the m-th array element
Ψ_Y	characteristic function
Ψ_c	characteristic function of a central χ^2 distributed random variable
$\psi_{ij,m}$	channel phase response from the m-th antenna element of user i to user j
Ψ_{nc}	characteristic function of a non-central χ^2 distributed random variable

σ	standard deviation
σ^2	variance
$\mathbf{h}$	channel gain vector
$\mathbf{n}$	noise vector
$\mathbf{r}$	received signal vector
$\mathbf{s}$	symbol vector
$\mathbf{w}$	beamforming weight vector
θ_m	phase difference between ϕ_m and ψ_m
$\widetilde{\gamma}_{best}$	best observed SNR
$\widetilde{\phi}_m$	observed phase rotation from the m-th array element
$\widetilde{\phi}_{best,m}$	best known phase perturbation
$\widetilde{w}_{best,m}$	best known beamforming weight
$\widetilde{X}_I$	imaginary part of the sum channel
$\widetilde{X}_R$	real part of the sum channel
a	step size
C	ergodic capacity
C_{RI}	covariance of $\widetilde{X}_R$ and $\widetilde{X}_I$
E_1	exponential integral function of the first order
F	cumulative distribution function
f	probability distribution function
F_k	non-central χ^2 cumulative distribution function
F_n	probability that the walker is less than a distance r from the starting point after n steps in random walk
f_n	probability distribution function for the end-to-end distance r in random walk
f_c	probability distribution function of a central χ^2 distribution

f_{nc}	probability distribution function of a non-central χ^2 distribution
H	sum channel
I	number of time intervals
I_α	α-th order modified Bessel function of the first kind
j_n	the m-th smallest positive zero of J_0
J_α	α-th order Bessel function of the first kind
K	confluent hypergeometric function
L	matrix size
M	number of active array elements
N	number of feedback bits per array element
n_r	number of receive antennas in the antenna array
O	starting point in random walk
p_e	bit error probability
P_N	noise power
p_u	common update probability
P_{mod}	error rate when modulation scheme is BPSK
P_{tx}	transmit power
Pr_{out}	outage probability
Q_l	generalized l-th order Marcum Q function
r	distance from the starting point
r_{max}	maximum distance after n steps
R_{sum}	sum-rate
s^2	non-centrality parameter
T_1	time duration of first hop sub-frame in a 2-hop system
T_2	time duration of second hop sub-frame in a 2-hop system
W_k	weighting factor

w_m	transmit weight that the m-th array element applies
X, Y, Z	random variables

1. Introduction

1.1 Motivation

The demand of data on mobile access networks has grown considerably in the last few years. At the same time, the number of devices that require connectivity is expected to grow at an exponential rate. Nowadays, numerous consumer electronics like smartphones, gaming devices, and television sets, are already networked, and by year 2020, it is predicted that we will be surrounded by an average number of 10 wireless-enabled devices, resulting in a ten-fold increase in the number of equipment with enabled wireless connectivity [1]. By the end of the decade, more than 50 billion connected devices are expected to be supported [2]. With chipset prices getting lower and lower, it seems that every piece of equipment and home appliance (with an appropriate source of power) will incorporate wireless connectivity as a basic feature in its design. Incorporated devices may also have different data requirements, but will be expected to be placed together in the near future. To cope with the growing demands, novel network architectures will be required [3].

Since conventional macrocell structure is not appropriate for providing high data rates in large coverage areas, the future mobile networks need to be heterogeneous, and should be able to support various network layers and different kinds of devices at the same time. A heterogeneous network (HetNet) is a mobile system composed of multiple types of access nodes, like macro-, micro-, pico- and femtocells. For example, for customers demanding wireless connectivity in a small apartment or office, one possible solution is to deploy a low-power femto base station (FBS) and provide connectivity to the core network of the service provider using, e.g., a residential digital subscriber line [4]. On the other hand, for corporate cus-

tomers that demand an adequate broadband coverage, the authors of [5, 6] suggested another option which consists of deploying a distributed architecture that relies on fiber optics (or power lines), to connect remote radio access units with a centralized processing unit.

As the majority of voice calls and data usage sessions take place inside buildings [7], the delivery of adequate indoor broadband coverage is crucial [8, 9]. The prevailing provision of indoor broadband wireless access from outdoor macro base station (MBS) is not a good option in practice since the high penetration losses caused by walls and floors put the indoor mobile stations (MS) in a very disadvantageous situation (i.e., the energy consumption required for the signal transmission is increased, decreasing the amount of information that can be transferred effectively). Heterogeneous systems, like the ones mentioned above, offer great improvements in the performance, but their implementation in practice comes with problems. For example, the coexistence of a large number of low-power FBSs and high-power MBSs in the same geographical area can generate substantial interference problems in the network. Furthermore, due to high expenses, the deployment of high quality (optical) backhaul might be only suitable for locations with high density of users like airports.

An interesting solution would be to combine the concepts of the aforementioned methods in [4] and [5, 6], and present a new approach to guarantee proper quality of service (QoS) for indoor users. That is, to boost the performance of an indoor MS by a massive cluster of (potentially wireless) cooperative network elements that are located in close proximity (i.e., in the same room or office) [II]. The use of distributed transmission schemes for wireless access networks is not completely new, and has been around for quite some time. For example, coordinated multi-point (CoMP) transmission and reception is a cooperation technique that has already been incorporated in LTE-Advanced. Transmission coordination in CoMP takes place among different cells, and improves the cell-edge capacity of the system. As a general, idea the abovementioned method is similar to CoMP, with two main differences: (a) the use of a wireless backhaul instead of a physical one, and (b) the participation of large number of low-cost low-power small access nodes instead of macrocell-sites.

A new approach is presented in this Thesis, where a cluster of relay stations (RSs) is applied. The RSs are separately distributed around the user in indoor environment, without a physical backhaul, and implement distributed beamforming (DBF). Distributed beamforming is a form of co-

operative communication, where various independent sources of information transmit simultaneously the same information to the intended destination. The basic idea behind this approach is to control the instantaneous phases (and sometimes also gains) of independent signal sources, to make them sum up constructively in reception. Distributed beamforming approach is appropriate for HetNet, where those mobile users that demand high data rates may use large number of radio-enabled devices in the environment as elements of a distributed antenna array. The potential benefits of deploying a DBF scheme are well known in the literature: full diversity benefit and M-fold power gain for M active array elements in the network [10].

1.2 Goals of the Research

We set the following goals for the research:

1. Design simple DBF algorithms that utilize minimum amount of feedback.

2. Analyze the performance of these DBF methods. For this purpose, we describe analytically the dependancy between performance, amount of feedback, and number of transmission nodes.

1.3 Research Justification

It is assumed that the cooperative network is composed by a large number of fixed low-cost RS (located on the walls and the ceiling of the room). The massive deployment of inexpensive RSs enables the implementation of a DBF scheme, providing an improvement in the *signal-to-interference-plus-noise* power *ratio* (SINR) of the different end-to-end wireless connections (i.e., boosting the desired signal energy at the destination, and mitigating the co-channel interference that is generated by neighbors). In other words, we may assume that an equivalent *distributed antenna system* (DAS) can be configured by using a common message in the first hop (from the main transmitter to RSs), and a DBF scheme with limited feedback in the second hop (from the RSs to a base station). It is assumed

that the bottleneck lies in the second hop, and that it can be improved by adjusting the channels (i.e., amplitudes and phases) that the main receiver sees from the antenna elements of each disperse RS. This enables the coherent combination of the multiple replicas of the original message at the intended destination.

The implementation of this cooperative cluster of RSs has many benefits. Obviously, range increases, power is saved and higher data rates are acquired through beamforming gain. In addition, the RSs are by definition low-cost and therefore do not consume much power. The implementation is bound to be cheaper than wired access points (that require a backbone connection), and the interference is expected to be less severe than with the deployment of FBSs (smaller radio range and power). Another benefit lies in the utilization of future HetNets, which are a mixture of different network elements. Different frequencies or even technologies (e.g. Wi-Fi) could be used in different hops (i.e., from transmitter to RSs and from RSs to receiver). Another example could a scenario where customers of different wireless broadband providers could be separated using different clusters of RSs at, for example, airports. Depending on the number of users per provider (at the time), the appropriate number of RNs could be assigned to serve the provider in question, and forward the signals toward the appropriate base station (BS). The resources of the first hop (from users to RNs) could be shared among users of different providers.

1.4 Structure of the Thesis

This Thesis is organized as follows. Fundamentals of cooperative communication are briefly discussed in Chapter 2. Chapter 3 presents the system model, the assumptions on the limited feedback DBF algorithm, and the differences between the two feedback models considered in this work. Chapter 4 provides a closed-form expressions for the signal-to-noise power ratio (SNR) distribution of the system, and then extends the analysis to the different performance measures that were selected for one feedback model. Chapter 5 shows numerical results that illustrate the effect of both, the amount of feedback bits per channel and the number of network elements in the selected performance criteria. Chapter 6 presents some possible improvements to the other feedback model, as well as results for the suggested extensions. Finally, conclusions are drawn, and some future resarch topics are presented in Chapter 7.

2. Fundamentals of Cooperative Communications

The use of cooperation has numerous advantages which will be briefly explained in this section. The power of radio signal decreases exponentially as the distance between a BS and its served mobile stations (MSs) increases. Mobile systems suffer from the cell edge problem, where the MSs near the BS can achieve high data rates, whereas the MSs on the cell edge can only get low data rate services.

Cooperative techniques like distributed (multi-user) multiple-input multiple-output (MIMO) show a promising ways to enhance the spectral efficiency of mobile communication systems. The performance gains of MIMO, and more recently cooperative techniques, have been well studied in the literature. In the above-mentioned methods, diversity and multiplexing gains translate into decreased transmission powers, higher capacity or better cell coverage. Another advantage is the more uniform QoS within the network. In traditional systems, users at the cell edge or in the shadowed areas suffer from capacity/coverage problems.

The use of relaying allows to balance this discrepancy and may give (almost) equal QoS to all users. It also allows the roll-out of systems that have minimal infrastructure available prior to deployment. Finally, a hybrid deployment of a cellular system coupled with RSs generally results in lowered capital and operational expenditures [11, 12].

In this chapter some fundamental concepts of cooperative communications are briefly presented. Starting from relaying, we proceed to the concept of heterogeneous network. Then, MIMO-based methods like DAS and (classical and distributed) beamforming are introduced.

2.1 Relaying Concepts

Relay nodes, or RSs as they will be referred in this work, play a central role in cooperative networks. They relay, as the name suggests, the received information to some pre-defined destination, usually after some simple operations on the way. The nature of the relaying can generally be classified into three groups:

- *Egoistic Behaviour (no help)*: Each RS communicates with the BS separately if there is data to transmit, or remains idle if there is no traffic to transmit. Other RSs can be considered as competitors. Therefore, the RSs with good channel conditions enjoy large rates, whereas RSs with a bad channel suffer from low rates.

- *Supportive Behaviour (unidirectional help)*: Data is delivered from a source towards a destination via RS(s) that do not have data of their own to transmit. The supporting RS is not gaining in performance at that particular instant, but benefits from the help of other supporting RSs when being in a situation of needing help.

- *Cooperative Behaviour (mutual help)*: The RSs are mutually helping each other. All involved RSs have data to transmit, and mutually try to get it successfully delivered. Cooperation smooths the impact of the wireless channel, such that even RSs in bad channel conditions experience an acceptable channel quality (and hence sufficient communication rates).

In Fig. 2.1, the three types of behaviour are exemplified. In addition, the relaying protocols can be classified into two groups: transparent and regenerative.

1. *Transparent relaying*: Does not modify the information represented by the applied waveform. Instead, some simple operations, like amplification and phase rotation, can be performed. Within this cathegory we can find:

   - *Amplify-and-Forward (AF)*: One of the simplest and most popular relaying methods, where the received signal is amplified, frequency trans-

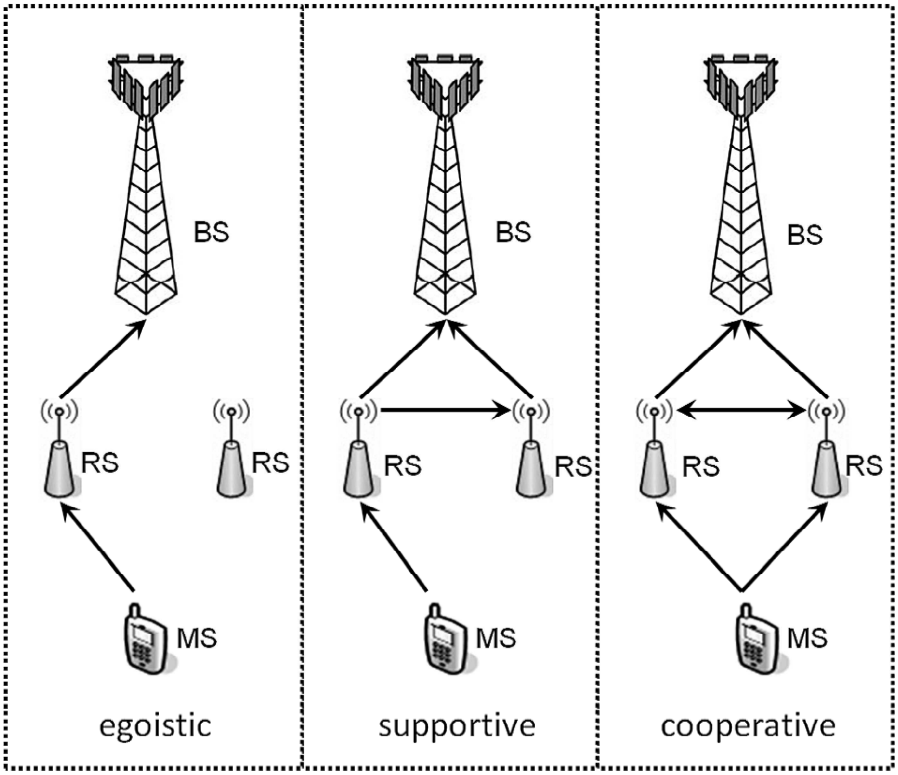

Figure 2.1. The typical relay station (RS) behaviours: egoistic, supportive, and cooperative types. The information is transmitted from a mobile station (MS) to a base station (BS) via one (or multiple) RS(s).

lated and retransmitted.

2. *Regenerative relaying*: Modifies the information (bits) or waveform (samples). It usually outperforms transparent relaying, but obviously also needs more powerful hardware. Within this cathegory we can find:

   - *Decode-and-Forward (DF)*: The prominent counter protocol to AF protocol, where the signal is detected, decoded, re-encoded and retransmitted.

In the rest of this Thesis, it is assumed that the RSs are low-cost, have fixed locations, and are equipped with one antenna. The same information is shared among all the RSs, and therefore, the nature of the relaying assumed for the system model in this Thesis is following the cooperative model. The relaying protocol is chosen to be DF because this relay type works better for large number of concurrently transmitting RSs [13]. It

can be generally stated that the higher is the level of cooperation, the better is the performance, but also the more complicated the setup and maintenance of the scheme [11].

2.2 Heterogeneous Network Approach

The shrinking of cell sizes through installation of additional macrocell-sites is no longer a sustainable solution to handle the traffic load in practice, especially as the indoor wireless traffic increases. To address the persistently increasing network capacity demand, deployment of smaller access points (that can form femto- or picocells), facilitate a better reuse of available spectrum. This shortens the communication links (by using less power), especially for indoor users, which in turn reduces the co-channel interference (CCI) level in the network. The reduction in cell size serves for two main purposes:

- maintain high SNR at the receiver while limiting the transmit power to moderate levels, and

- reduce the number of users per cell.

Lower transmit powers and smaller number of users per cell result in reduction of interference level, which directly translates into capacity enhancement in the system, but also leads into new forms of interference, such as cross-layer interference between femto- or picocell access nodes and macrocell users. In addition to femto- and picocells, the dense deployment of transmission points can be faced in sensor and relay systems. The challenge is how to maximize coverage of the (low-power) RSs (or sensors), which can coordinate the radio cooperations with each other, or equivalently, how to minimize the number of RSs to cover a given area. These coexistence problems are addressed under the umbrella term heterogeneous networks.
Heterogeneous network is a system composed by multiple types of access nodes in a wireless network, and it may operate using a single wireless standard, like Third Generation Partnership Project's (3GPP) Long Term Evolution (LTE), and LTE-Advanced for the universal mobile telecommunications system (UMTS). Previously, term HetNet has also been used to refer the cooperative coexistence of different wireless technologies.

By forming a hierarchical cellular network, HetNet aims to improve the network performance by coordinating the resource allocation and service delivery, using nodes with different transmission capabilities within a given cell; i.e., access nodes have different radio frequency (RF) capabilities, ranging from macro- to femto- and picocell scales. For example, in LTE-Advanced, HetNet may be comprised of a macrocell associated with an enhanced Node B (eNB), and a number of lower power access nodes, such as femto and pico home eNBs (HeNB) [6, 14]. The interference problems, namely cross-layer and co-layer interference problems, are further addressed in the Future Work section of Chapter 7.

2.3 Multi-Antenna Techniques

Systems with multiple antennas at the transmitter and receiver are called MIMO systems. The multiple antennas can increase spectral efficiency through multiplexing, or improve performance through diversity.

- *Diversity Gain*: Each pair of transmit and receive antennas provide a signal path from the transmitter to the receiver. More reliable reception is achieved by sending signals that carry the same information through different paths, so that multiple independently faded replicas of the data symbol are obtained at the receiver. For example, in a slow Rayleigh-fading environment with one transmitter and n receive antennas, the transmitted signal is passed through n different paths, which results in a maximal diversity gain of n. Respectively, in a system with m transmit and n receive antennas (where the path gains between individual antenna pairs are *independent and identically distributed* Rayleigh faded) the maximal diversity gain is $m \times n$. Diversity is a powerful technique to mitigate fading in wireless links.

- *Spatial Multiplexing Gain*: Another line of thought is that fading in a MIMO channel can be utilized through increased degrees of freedom available for communication. If the path gains between the individual transmit-receive antenna pairs fade independently, then the channel matrix is with a high probability well conditioned, and is able to support multiple parallel spatial channels. This so-called *spatial multiplexing* increases the data rate. In a case of m transmit and n receive antennas, it is possible to show that the available degree of freedom is $\min(m, n)$.

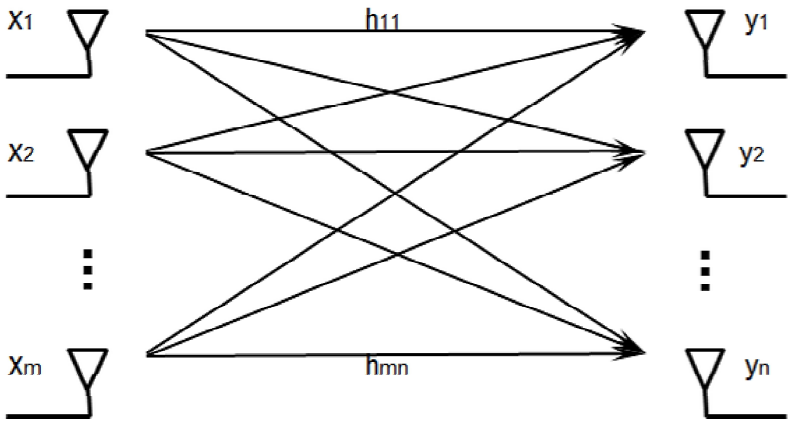

Figure 2.2. A generalized model of a multi-antenna system with m transmit antennas and n receive antennas.

Since the data throughput and link range can be increased without additional bandwidth or transmit power, MIMO technology has become one of the popular forms of smart antenna technology. The acquired spectral efficiency gains require, however, accurate knowledge of the channel at the receiver side (and sometimes at the transmitter side). The cost of performance improvements is the added cost of deploying multiple antennas, demanding more physical space and circuit power requirements, and the added complexity of the system. Figure 2.2 shows a MIMO system with m transmit antennas and n receive antennas. The single-user MIMO only considers the antennas that are physically connected to the terminal, whereas distributed MIMO exploits the availability of multiple independent radio terminals utilizing beamforming [15, 16, 17].

2.3.1 Beamforming

Beamforming is an array signal processing method which increases SNR through coherent combination of channels. The term "beamforming" derives from the fact that early spatial filters were designed to form pencil beams (see polar plot in Fig. 2.3) to receive (or transmit) signal radiation from a specific location, and attenuate signals from other locations [18]. This is achieved by combining the elements in the arrays in such way that the signals at particular angles experience either constructive or destructive summation.

Even though the focus in this Thesis is on the broadband wireless mobile systems, for the sake of clarification, the two figures presented here are taken from sources dealing with the beamforming in the radar technology. The basic idea is the same, but the features in the polar plots are

more prominent. In Fig. 2.4, a beamforming pattern of a two-antenna array with $n_r = 4$ receive antennas is depicted. There are two symmetrical main lobes and four sidelobes. In Fig. 2.3, the beams in unwanted directions are nulled and only a pencil beam in the desired direction (with some sidelobes) is retained. To generate a steerable beam from a phased-array, the following three main functions have to be accomplished:

- Co-phase the signals arriving at the elements of the array from/to the desired direction.

- Apply amplitude weighting to control the spatial sidelobe structure.

- Sum the weighted co-phased signals to produce the wanted beam.

The wavefront, arriving from a direction other than bore-sight, will reach different elements of the array at different times depending on their position. Therefore, the most logical method for co-phasing would be to introduce variable time-delays into the elements outputs. However, it is sometimes impractical to provide the beam steering via time-delays. Therefore, another option is to approximate the time-delays by a phase-shift. As an example, three beamforming techniques are briefly presented here:

1. *Null steering beamforming algorithm*: Forms a beam towards the desired direction and nulls the interference in selected directions.

2. *Minimum variance distortionless response (MVDR) beamforming algorithm*: Does not require the knowledge of the directions of the interference for weight calculation. Only the direction of the desired signal is required. The beamforming weights are selected by minimizing the mean output power while maintaining unity response in the main beam direction.

3. *Minimum mean square error (MMSE) beamforming algorithm*: Utilizes a reference signal, which is correlated to the desired signal and uncorrelated with interfering signals. In multipath fading environment it gives the optimum results.

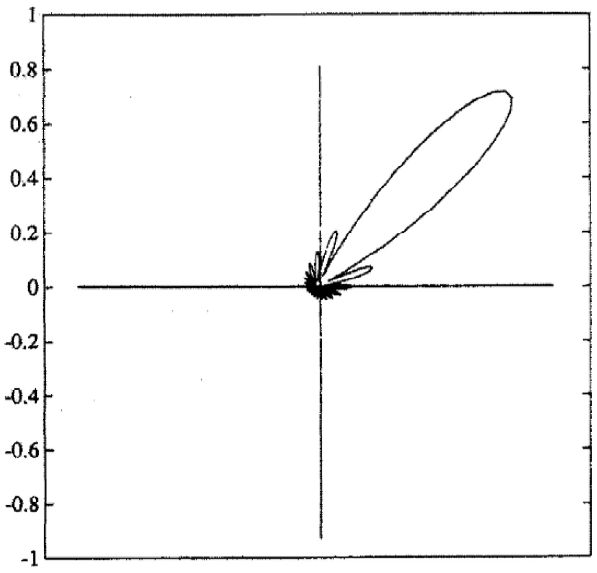

Figure 2.3. A polar plot for beamforming, where the beamformed pencil beam is aimed at the desired direction [18].

Depending on the application requirements, usually one of these beamforming algorithms is selected [19, 20].

2.4 Distributed Antenna Systems

Distributed antenna system refers to a (multi-user) MIMO concept comprising multiple antennas co-located at one end of the radio link, and several geographically scattered access points (APs) (with multiple antennas) at the other end. Therefore, the inherent macrodiversity, due to widely spaced antennas, offers the capability to enhance signal quality, increase system capacity, and improve coverage [22].

Distributed antenna systems were originally proposed to improve the indoor coverage performance of wireless communication systems, but they have been recently considered also in academic publications as well as in standardization activities, as a cooperative communication technique. The original idea of DAS was to provide coverage for an entire building (or a large section of the building), from a single BS located in the building. Thus, instead of one high power antenna, a group of low-power antenna elements are used to cover the area with reduced total power, and improved reliability [23].

In [24], the benefits of deploying DAS in in-building multi-floor propagation environments are presented. Buildings represent challenging environments consisting of a complex mixture of strong line-of-sight (LOS)

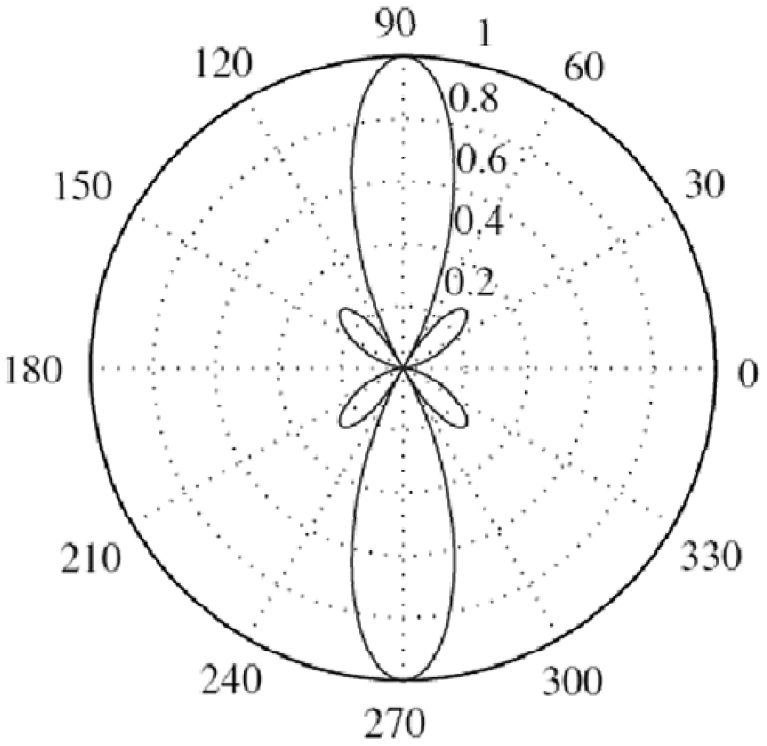

Figure 2.4. A polar plot for beamforing, where the receive beamforming pattern is aimed at 90^{o}, with two-antenna array and $n_r = 4$ receive antennas [21].

and non-line-of-sight (NLOS) propagation, affected by factors like walls, floors, and even architectural styles. In addition, the signal paths generated by reflection and transmission within the building may increase the level of co-channel interference. In Fig. 2.5, an uplink transmission model is shown in a multi-storey building scenario. Each floor represents a cell equipped with evenly spaced, multiple ceiling mounted remote antenna units (RAUs), which are located in the same positions on every floor, to serve all MSs located at each floor. The RAUs are connected to a central unit (CU) (also called as baseband processing unit), where the transmitted/received signals are constructively processed. The same frequencies are reused on adjacent floors, but not within the same floor. Therefore, there are two possible sources of interference:

1. Direct signal transmissions through the floor partitions, and

2. Transmissions that involve signal reflections and scattering from outdoors (i.e., from nearby building or outdoor BS).

In [24], the use of in-building DAS has been proven to support a high number of MSs on the same frequency, and to provide high data rates

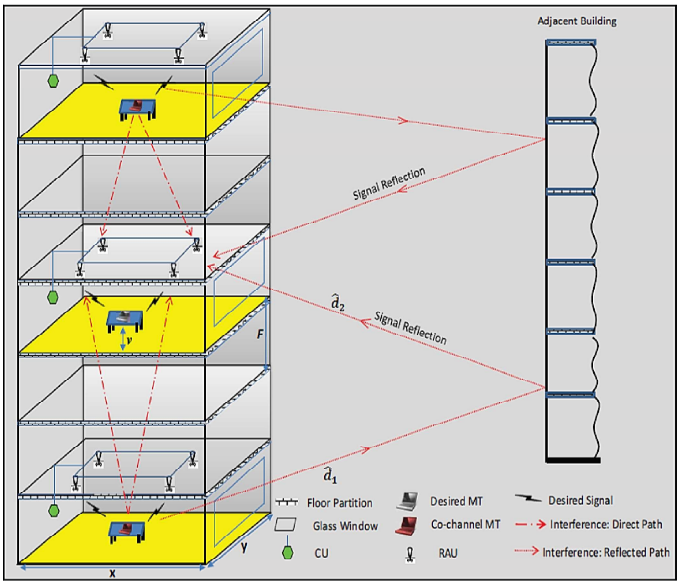

Figure 2.5. In-building DAS with frequency reuse in every floor. There are U central units (CUs) which consist of N remote antenna units (RAUs) each, and a multistory building is located a few meters away [24].

for indoor MSs. The results are also informative from the perspective of indoor femtocell systems, which are one of the most promising future in-building mobile communication system architectures.

2.4.1 Distributed Beamforming

Wireless MIMO systems that use beamforming techniques are able to provide notable improvements to information rate and transmission reliability of mobile communication systems. Due to the cost and implementation issues, however, it is practically challenging to employ multiple antennas in wireless communication systems. Instead of using highly sophisticated transceivers, the transmit beamforming algorithm can be implemented by using antennas belonging to different single-antenna equipment.
Distributed beamforming is a technique where a RF signal is transmitted over multiple antennas/single-antenna devices, like simple RSs. Transmission from different antennas/RSs are coordinated, such that component signals sum up coherently in the direction of the intended destination (i.e., system is forming a virtual multi-antenna array) [25, 26]. Digital beamforming is based on converting the RF signals into two streams of binary baseband in phase (I) and quadrature (Q) signals, which jointly represent the amplitudes and phases of signals transmitted/received at the elements of the array. The beamforming is carried out by adjusting the amplitudes and phases (through weighting the digital signals), so that

when added together they form the desired beam [27].

Especially in case of relaying, the use of multiple RSs to form a virtual array is challenging: due to the physical separation of RSs, they only have access to the channel state information (CSI) of their own links in the second hop. Furthermore, the RSs must agree on message transmission time, the carrier synchronization, and the carrier phases that guarantee a constructive combination of the signals at the destination. Therefore, the proper implementation of the concept requires the development of implementable distributed techniques for information sharing, timing synchronization and carrier synchronization. With proper implementation, distributed beamforming has the potential of attaining considerable improvement in range, rate, or power efficiency [10, 26].

Cooperative DAS has drawn much attention in both academic research and standardization activities, like 3GPP, LTE and LTE-Advanced, where it is referred as CoMP transmission. In Fig. 2.6, the traditional cellular system and cooperative DAS cellular model are compared. For simplicity, an omnidirectional cellular system is considered. In the traditional mobile cellular system, all antennas of a BSs are located in the center of the cells, while in the cooperative DAS mode multiple antennas of a BS (i.e., RAUs) are distributed in the cell. The RAUs are connected to a baseband processing unit (BPU) by using high-quality bidirectional wired or wireless links. The use of DAS improves the system coverage, as the transmitted signals are more uniformly distributed over the cells, and the exhaustion of radio signal energy is alleviated due to the decreased average distance from the MSs to the RAUs. The DAS can also form an intracell CoMP system (distributed MIMO), employing several RAUs at different geographical locations [12].

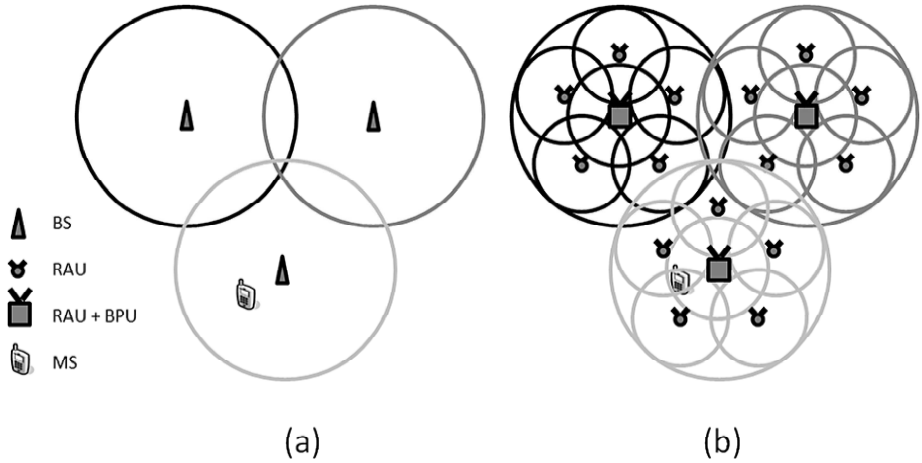

Figure 2.6. Traditional cellular and cooperative DAS cellular models: a) Traditional cellular model, where the mobile station (MS) is supported by a base station (BS); b) cooperative DAS cellular model, where the remote antenna units (RAUs) of the BS are distributed in the cell, and connected to a baseband processing unit (BPU) located in the center of the cell.

3. System Model

The system model, and the signal model for the proposed cooperative relaying system are presented in this chapter, with the assumptions on the limited feedback DBF algorithm. A generalized layout of the system is illustrated in Fig. 3.1. The system consists of a main transmitter, a main receiver, and a cluster of M active RSs that provide the array elements of the DBF approach that is implemented in the second hop. All devices are equipped with a single transmit/receive antenna. The model is the same as presented in Publications I and II. In the proposed system model, main transmitter and the RSs in the cluster operate in a half-duplex mode, in a DF fashion. Thus, during the first hop of duration T_1, message intended for the main receiver is sent from main transmitter to the nearby array elements (i.e., the antennas of the distributed RSs). During the second hop of duration T_2, the message is sent from the array elements to the main receiver. In the simplest case, where the array elements share the same physical space with the main transmitter (e.g., same room or office), the attenuation on the first link is assumed to be small, and channel is either static or slowly varying (e.g., LOS channel model). This makes possible to assume that communication on the first link can be accomplished with (almost) no cost in terms of power and/or time. However, if the array elements are distributed in a different geographical location w.r.t. the main transmitter (e.g., in different rooms), the penetration losses caused by the walls and floors would increase the cost of communication in the first hop. Nevertheless, the longer distance that exists between the clustered array elements and the main receiver implies a large attenuation in the links of the second hop, when compared to the attenuations in the first hop. This situation makes the second hop the bottleneck of the system, and its analysis is the main goal of this Thesis.

A more detailed system model, when the first hop takes place inside a

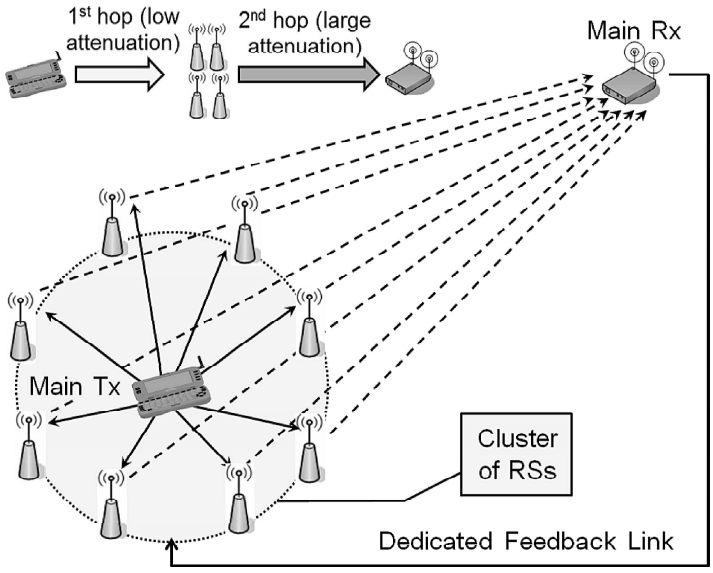

Figure 3.1. Generalized system model composed by a main transmitter, a main receiver, and a cluster of relaying network elements (around main transmitter). The feedback link between main receiver and relaying cluster enables the implementation of distributed beamforming in the second hop.

room, is depicted in Fig. 3.2, where a low-rate, reliable, and delay-free feedback channel exists between the main receiver and the active array nodes. Main receiver uses this channel to convey a quantized version of the phase adjustment that each element of the antenna array should apply in transmission (to maximize SNR in reception). In other words, the limited feedback information that the main receiver reports is used to establish a DAS in the second hop. Multiple active array elements transmit cooperatively at the same time, focusing the resulting beam towards the direction of the intended destination over the second hop.

3.1 Signal Model

Based on the above model, the received signal at transmission time interval i attains the (dot product) form

$$\mathbf{r}[i] = (\mathbf{h}[i] \cdot \mathbf{w}[i])\, \mathbf{s}[i] + \mathbf{n}[i] = H[i]\mathbf{s}[i] + \mathbf{n}[i], \tag{3.1}$$

where $\mathbf{h}[i]$ is the channel gain vector, $\mathbf{w}[i]$ is the beamforming weight vector, $H[i] \in \mathbb{C}^{1\times 1}$ is the resulting sum channel, $\mathbf{s}[i] \in \mathbb{C}^{1\times \mathrm{L}}$ is a vector that contains L complex modulation symbols, and $\mathbf{n}[i] \in \mathbb{C}^{1\times \mathrm{L}}$ refers to an *additive white Gaussian noise* (AWGN) sample with power P_N. Power control is not applied in the array elements and thus, the total transmit power P_{tx} in the second hop remains fixed during the whole duration of the com-

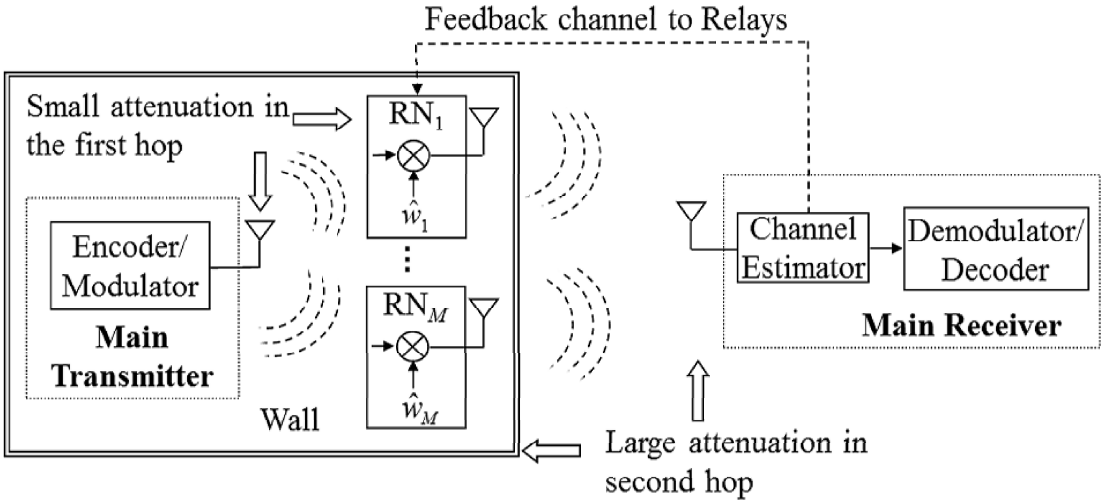

Figure 3.2. A more detailed system model composed by a main transmitter, a main receiver, and a cluster of M RSs, where the first hop takes place indoors.

munication.

In case of unitary noise power (i.e., $\mathbb{E}\left\{\mathbf{n}[i]^T\mathbf{n}[i]^*\right\}$ is the identity matrix of size L), the received SNR in the second hop is given by

$$\gamma[i] = \Big|\sum_{m=1}^{M}\sqrt{\gamma_m[i]}\,w_m[i]e^{j\psi_m[i]}\Big|^2, \tag{3.2}$$

where $\gamma_m[i]$ represents the received SNR from the m-th array element, $\psi_m[i]$ is the corresponding channel phase response, and $w_m[i]$ is the transmit weight that the m-th array element applies.

3.2 Assumptions on System Model

In our system, the instantaneous SNR value in (3.2) is assumed to be time-invariant in a time scale proportional to the duration of a data session, since all RSs in the second hop admit a fixed location. Thus, the channel is considered not to change significantly in time and, therefore, $\gamma_m[i] = \gamma_m$, $\psi_m[i] = \psi_m$ is used. Based on the time invariant nature of the system, also the time index i of the weights $w_m[i]$'s, which are used to make phase adjustments at the m-th element of the antenna array, can be ignored. In presence of channel gains that remain static during the whole duration of the data session, the feedback message for phase adjustments at the different RSs can spread over an appropriate time span, denoted by $i = 1, 2, \ldots, \mathcal{I}$. So, the presented performance analysis considers the resulting sum channel when all the phase adjustments have been appropriately performed (i.e. after $\mathcal{I}$ time intervals of the sequential DBF algorithm that is implemented).

It is also assumed that phases ψ_m are independent and identically distributed (i.i.d.) uniform *random variables* (RVs) that take values on interval $(-\pi, \pi)$. The performance of the proposed DBF algorithm is studied assuming a random initial phase configuration (i.e., with no *a priori* information). To fulfill the accurate timing requirements at each element of the disperse antenna array, we assume that each RS in the cluster is able to monitor standard synchronization signals either from destination (i.e., main receiver) in the reverse link, or from the source (i.e., main transmitter) in the forward link.

The signal phase shifts that the array elements apply easily create frequency selectivity, which is seen as an increased multipath effect in the resulting wireless channel. Yet, in our system model we assume that the synchronization error of the array elements is small when compared to symbol length. As a consequence, delay spread of the effective channel will not be (considerably) increased in this situation.

3.3 Feedback Approaches

In this Thesis, two slightly different system models are considered. What sets them apart is the type of feedback channel they utilize. The main focus of the Thesis is the dedicated feedback channel approach, where each RS has its own individual CSI feedback channel. The second model utilizes a common CSI feedback scheme, that, on the other hand, has only one common low-rate feedback channel among all the RSs.

- In dedicated feedback approach, channels between receiver and each RS in the cluster are known at the receiver. Thus, RSs should apply mutually orthogonal reference signals that are used in the main receiver for channel estimation. Based on this channel knowledge, the main receiver can provide dedicated feedback to each RS.

- In common feedback approach, the main receiver cannot separate transmissions from different RSs, and it can provide only feedback based on detected sum signal. Therefore, the dedicated feedback is not meaningful, and single common feedback message is sent to main transmitter or cluster of RSs.

We note that amount of dedicated feedback is growing linearly with the number of RSs in the cluster, while the amount of feedback per channel use is not depending on the number of RSs. The main part of the Thesis is focuses on the dedicated feedback approach, with the exception of Chapter 6, where the common feedback approach is briefly touched upon.

4. Performance Analysis

In the rest of the Thesis we assume that RF carriers of the RSs are synchronized, and the estimation of each individual channel gain that the main receiver observes in the second hop is ideal. The analytical results for the individual feedback scheme can then be obtained with the aid of the central limit theorem, to approximate the SNR distribution. The analysis of this section is based on the Publications I and II.

4.1 Individual Feedback Channel

As shown in Chapter 3, we assume that in the second hop of the communication link there are M active array elements, each one transmitting the same stream of complex symbols to the main receiver. In order to maximize the SNR at the main receiver, each array element adjusts its transmission using a complex, individual beamforming weight

$$w_m = \sqrt{\frac{P_{\text{tx}}}{M}}\, e^{-j\phi_m}, \quad \phi_m \in \mathcal{Q}, \quad \mathcal{Q} = \left\{ \frac{2\pi(n-1)}{2^N} : n = 1, \ldots, 2^N \right\} \tag{4.1}$$

We note that the individual power per antenna (i.e., $|w_m|$) is selected based on the number of active array elements; therefore, the total transmit power in the system is set to P_{tx}, which makes the fair comparison in the presented results possible. The error-free signaling indicating the best phasing index n, is provided through the dedicated feedback channel. Note that the number of feedback bits per array element is N.

Phases ϕ_m are selected in the main receiver as follows:

1. Receiver first estimates the channel phases ψ_m from each element of the distributed antenna array, using antenna specific reference signals.

2. Then, receiver selects the phases ϕ_m from quantization set $\mathcal{Q}$, such that $|\theta_m| = |\phi_m - \psi_m|$ is minimized.

The adjusted phases θ_m are i.i.d. and uniformly distributed in the interval $(-\frac{\pi}{2^N}, \frac{\pi}{2^N})$ [28]. Thus, phase adjustments are done independently, using a common phase reference at the receiver side.

Three different performance measures are presented: outage capacity, ergodic capacity, and bit error probability. Before the performance analysis can be carried out, we need to determine suitable expressions for the *probability density function* (PDF) and the *cumulative distribution function* (CDF) of the received instantaneous SNR. According to the system model presented in Chapter 3, the expression for SNR attains the form

$$\gamma[i] = |H[i]|^2 = \frac{P_{\text{tx}}}{M}\left|\sum_{m=1}^{M}\sqrt{\gamma_m}e^{j\theta_m[i]}\right|^2, \tag{4.2}$$

where individual received SNRs $\{\gamma_m\}_{m=1}^{M}$ are known, and remain constant due to transmitter and receiver having fixed locations. Since we want to analyze the effect of the feedback signaling resolution (i.e., N) and the number of elements in the antenna array (i.e., M) in the performance of the DBF system, suitable expressions for the conditional PDF $f\left(\gamma[i]|\gamma_1,\ldots,\gamma_M\right)$ and CDF $F\left(\gamma[i]|\gamma_1,\ldots,\gamma_M\right)$ are required. Unfortunately, a treatable closed-form expression for these distributions can only be obtained for very specific situations (i.e., not for all values of M and N). However, since we are interested in studying the performance measures when the number of elements in the DAS is high (i.e., when $M \geq 10$), we can use the central limit theorem to show that RV (4.2) can be accurately approximated as the sum of two independent *chi-squared* (χ^2) RVs (one central and one non-central), each with one degree of freedom.

4.1.1 Central and Non-Central Chi-Square Distributions

Let $\{X_l\}_{l=1}^{n}$ be independent Gaussian RVs with common variance σ^2 and non-negative mean μ_l. Then, sum

$$Y = \sum_{l=1}^{n} {X_l}^2 \tag{4.3}$$

follows a *non-central* χ^2 distribution with n degrees of freedom [29]. The corresponding PDF expression is given by

$$f_{nc}(y) = \frac{1}{2\sigma^2}\left(\frac{y}{s^2}\right)^{\frac{n-2}{4}}\exp\left(-\frac{s^2+y}{2\sigma^2}\right)I_{\frac{n}{2}-1}\left(\frac{s}{\sigma^2}\sqrt{y}\right) \quad y \geq 0, \tag{4.4}$$

where

$$s^2 = \sum_{l=1}^{n} \mu_l^2 \tag{4.5}$$

is the non-centrality parameter of the distribution, and

$$I_\alpha(x) = \frac{1}{\pi} \int_0^\pi \cos(\alpha\theta) \exp(x \cos\theta) d\theta \tag{4.6}$$

is the α-th order modified Bessel function of the first kind [30]. The characteristic function of a non-central χ^2 distribution can be defined in closed-form, and it is given by

$$\Psi_{nc}(\omega) = \left(\frac{1}{1 - 2j\omega\sigma^2}\right)^{\frac{n}{2}} \exp\left(\frac{j\omega s^2}{1 - 2j\omega\sigma^2}\right). \tag{4.7}$$

We note that in the particular case when all means are zero (i.e., when $\mu_l = 0$ for $l = 1, \ldots, n$), the distribution of RV (4.3) reduces to the so-called *central* χ^2 distribution, whose PDF expression for n degrees of freedom is given by

$$f_c(y) = \frac{1}{2^{\frac{n}{2}} \Gamma\left(\frac{n}{2}\right) \sigma^n} y^{\frac{n}{2}-1} \exp\left(-\frac{y}{2\sigma^2}\right) \qquad y \geq 0, \tag{4.8}$$

where

$$\Gamma(y) = \int_0^\infty t^{y-1} \exp(-t) dt \tag{4.9}$$

represents the Gamma function [29]. Then, the corresponding characteristic function in this situation is given by

$$\Psi_c(\omega) = \left(\frac{1}{1 - 2j\omega\sigma^2}\right)^{\frac{n}{2}}. \tag{4.10}$$

Let us now assume that

$$Z = Y_1 + Y_2 \tag{4.11}$$

is the combination of two independent χ^2 RVs: A non-central χ^2 RV with non-centrality parameter ${s_1}^2$ and variance ${\sigma_1}^2$, and a central χ^2 RV with variance ${\sigma_2}^2$, respectively. Let us also consider that the degrees of freedom are equal (i.e., $n_1 = n_2 = m$). A typical way to obtain the distribution of RV Z is to calculate its characteristic function [31], i.e.,

$$\Psi_Z(\omega) = \left[\frac{1}{(1 - 2j\omega{\sigma_1}^2)(1 - 2j\omega{\sigma_2}^2)}\right]^{\frac{m}{2}} \exp\left(\frac{j\omega {s_1}^2}{1 - 2j\omega{\sigma_1}^2}\right), \tag{4.12}$$

which then can be inverse-Fourier transformed to yield the PDF

$$\begin{aligned} f_Z(z) &= \frac{1}{2{\sigma_1}^2} \left(\frac{\sigma_1}{\sigma_2}\right)^m \left(\frac{z}{{s_1}^2}\right)^{\frac{m-1}{2}} \exp\left(-\frac{z + {s_1}^2}{2{\sigma_1}^2}\right) \\ &\times \left[\sum_{k=0}^{\infty} \frac{\Gamma\left(\frac{m}{2} + k\right)}{\Gamma(k+1)\Gamma\left(\frac{m}{2}\right)} \left(\frac{\sqrt{z}\left({\sigma_2}^2 - {\sigma_1}^2\right)}{s_1 {\sigma_2}^2}\right)^k \right. \\ &\times \left. I_{m+k-1}\left(\frac{\sqrt{z} s_1}{{\sigma_1}^2}\right)\right] \qquad z \geq 0. \end{aligned} \tag{4.13}$$

Finally, it is possible to show that the CDF in this situation admit the form

$$\begin{aligned} F_Z(z) &= \left(\frac{\sigma_1}{\sigma_2}\right)^m \sum_{k=0}^{\infty} \frac{\Gamma\left(\frac{m}{2}+k\right)}{\Gamma(k+1)\Gamma\left(\frac{m}{2}\right)} \left(\frac{{\sigma_2}^2-{\sigma_1}^2}{{\sigma_2}^2}\right)^k \\ &\times \left[1-Q_{m+k}\left(\frac{s_1}{\sigma_1},\frac{\sqrt{z}}{\sigma_1}\right)\right] \qquad z \geq 0, \end{aligned} \tag{4.14}$$

where

$$Q_l(a,b) = \int_b^{\infty} x \left(\frac{x}{a}\right)^{l-1} \exp\left(-\frac{x^2+a^2}{2}\right) I_{l-1}(ax)\, dx \tag{4.15}$$

is the generalized l-th order Marcum Q function [29].

4.1.2 PDF and CDF Approximations in Case of Large Number of Array Elements

Due to the Euler's formula, the RV

$$H[i] = \widetilde{X}_R[i] + j\widetilde{X}_I[i] \tag{4.16}$$

can be written in terms of its real and imaginary parts:

$$\widetilde{X}_R[i] = \sqrt{\frac{P_{tx}}{M}} \sum_{m=1}^{M} \sqrt{\gamma_m} \cos\theta_m[i], \tag{4.17}$$

$$\widetilde{X}_I[i] = \sqrt{\frac{P_{tx}}{M}} \sum_{m=1}^{M} \sqrt{\gamma_m} \sin\theta_m[i]. \tag{4.18}$$

Based on the fact that M is *large*, we refer to the central limit theorem to justify that both, real and imaginary parts of $H[i]$ are Gaussian with means μ_R and μ_I, respectively [31]. Since the imaginary part of $H[i]$ is a sum of sine functions with symmetrically distributed phases, its mean equals zero[1]. Based on the discussion presented in Section 4.1.1, we observe that RV $|\widetilde{X}_I[i]|^2$ can be approximated using a central χ^2 distribution with 1 degree of freedom. Similarly, we find that the expected value of the real part of $H[i]$ is non-negative (actually, $\mu_R = 0$ only when $N = 0$). So, we claim that the distribution of RV $|\widetilde{X}_R[i]|^2$ can be approximated as a non-central χ^2 distribution with 1 degree of freedom and some non-centrality parameter ${s_1}^2$ (unknown for the moment).

One final detail needs to be checked, before we can form approximation for modeling the probabilistic behavior of main receiver's SNR (i.e., $\gamma[i]$): we need to show that the real and imaginary parts of $H[i]$ (i.e., $\widetilde{X}_R[i]$ and $\widetilde{X}_I[i]$) are independent RVs. In this particular case, since $\widetilde{X}_R[i]$ and $\widetilde{X}_I[i]$

[1] Individual phases $\theta_m[i]$ are uniformly i.i.d. on interval $(-\frac{\pi}{2^N}, \frac{\pi}{2^N})$ for all m, and sine is an odd function.

are modeled as Gaussian distributed RVs (due to, we are calling the central limit theorem), independence requirement is guaranteed if correlation coefficient between both RVs equals zero [31]. Fortunately, it is possible to show that this condition is satisfied, since for the covariance of $\widetilde{X}_R[i]$ and $\widetilde{X}_I[i]$ holds

$$C_{RI} = \mathbf{E}\{\widetilde{X}_R[i]\widetilde{X}_I[i]\} - \mathbf{E}\{\widetilde{X}_R[i]\}\,\mathbf{E}\{\widetilde{X}_I[i]\} = 0. \tag{4.19}$$

Finally, the parameters that are required for the approximations of PDF and CDF can be obtained from the first two raw moments of RVs $\widetilde{X}_R[i]$ and $\widetilde{X}_I[i]$, after simple but tedious computations:

$$\mu_R = \sqrt{\frac{P_{tx}}{M}}\, C_N \sum_{m=1}^{M} \sqrt{\gamma_m}, \qquad \mu_I = 0, \tag{4.20}$$

$$\begin{aligned} \mathbb{E}\left\{\widetilde{X}_R^2\right\} &= \frac{P_{tx}}{M}\left[\sum_{m=1}^{M} \gamma_m \left(\frac{1}{2} + \frac{1}{2}C_{N-1}\right)\right. \\ &+ \left. 2\sum_{l=1}^{M-1}\sum_{m=l+1}^{M} \sqrt{\gamma_l}\sqrt{\gamma_m}\, {C_N}^2\right], \end{aligned} \tag{4.21}$$

and

$$\mathbb{E}\left\{\widetilde{X}_I^2\right\} = \frac{P_{tx}}{M}\sum_{m=1}^{M} \gamma_m \left(\frac{1}{2} - \frac{1}{2}C_{N-1}\right), \quad C_N = \frac{2^N}{\pi}\sin\left(\frac{\pi}{2^N}\right). \tag{4.22}$$

As shown in Section 4.1.1, when the degrees of freedom are both one ($m = 1$), the PDF for the DBF scheme ($Z = |X_R|^2 + |X_I|^2$) can be expressed as a weighted sum of non-central χ^2 distributed PDFs, with $\sigma = \sigma_1$ and $n = 2(k+1)$, i.e.,

$$f_Z(z) = \sum_{k=0}^{\infty} W_k(\sigma_1, \sigma_2) f_k(z), \tag{4.23}$$

where

$$\sigma_1 = \sqrt{\mathbb{E}\left\{\widetilde{X}_R^2\right\} - \mu_R}, \qquad \sigma_2 = \sqrt{\mathbb{E}\left\{\widetilde{X}_I^2\right\}}, \tag{4.24}$$

are the standard deviations of the real and imaginary parts, respectively,

$$W_k(\sigma_1, \sigma_2) = \frac{\sigma_1}{\sigma_2}\frac{\Gamma\left(\frac{1}{2}+k\right)}{\Gamma(k+1)\Gamma(\frac{1}{2})}\left(\frac{\sigma_2^2 - \sigma_1^2}{\sigma_2^2}\right)^k \tag{4.25}$$

is the corresponding weighting factor, and

$$f_k(z) = \frac{1}{2\sigma_1^2}\left(\frac{z}{s_1^2}\right)^{\frac{k}{2}} \exp\left(-\frac{s_1^2 + z}{2\sigma_1^2}\right)\mathcal{I}_k\left(\frac{s_1}{\sigma_1^2}\sqrt{z}\right) \qquad z \geq 0 \tag{4.26}$$

is the non-central χ^2 PDF as defined in (4.4). As seen in Fig. 4.1, the values of the weighting factor are decaying rapidly with k; i.e., only a few

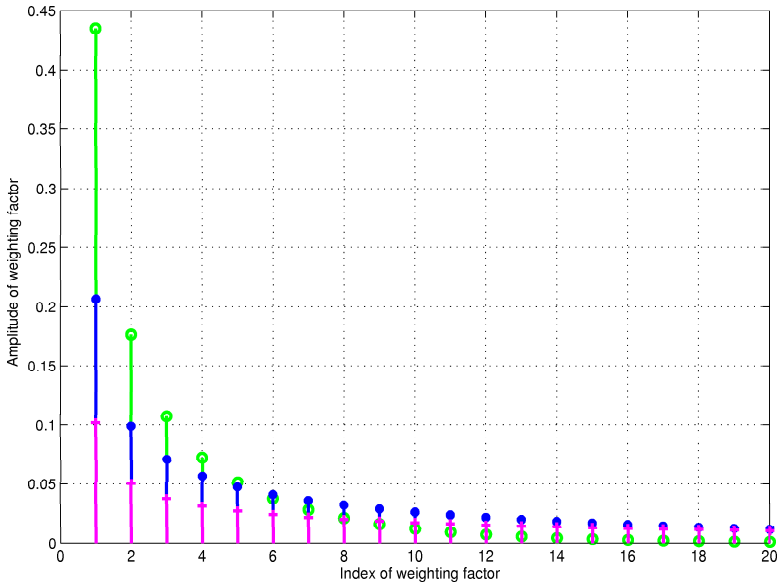

Figure 4.1. Amplitude of different weighting factor $W_k(\sigma_1, \sigma_2)$'s, used to approximate the PDF/CDF of received SNR $\gamma[i]$ as a weighted sum of non-central χ^2 PDFs/CDFs with different degrees of freedom. Channel phase resolutions [bit/RS]: $N = 1$ ('o'), $N = 2$ ('•'), and $N = 3$ ('+').

terms of the sum in (4.23) are needed to obtain an accurate approximation for the resulting PDF.

Following a similar procedure, the corresponding CDF for the received SNR can be expressed as a weighted sum of non-central χ^2 CDFs, i.e.,

$$F_Z(z) = \sum_{k=0}^{\infty} W_k(\sigma_1, \sigma_2) F_k(z), \tag{4.27}$$

where

$$F_k(z) = 1 - Q_{k+1}\left(\frac{s_1}{\sigma_1}, \frac{\sqrt{z}}{\sigma_1}\right) \tag{4.28}$$

is the non-central χ^2 CDF.

4.2 Performance Analysis of Distributed Beamforming with Limited Feedback

In this Thesis, three different performance measures are computed for the dedicated feedback channel scheme [32]:

1. **Ergodic capacity:** Represents the long-term average transmission rate, and can be achieved implementing coding schemes that span code words over several coherence time intervals of the fading channel. This performance measure is valid for applications that do not have strict

delay constraints.

2. **Outage capacity:** Constitutes a more appropriate performance indicator in case of constant-rate delay-limited transmissions, where coding must be carried out over a single channel realization. Represents the maximum constant rate that can be maintained for a given outage probability.

3. **Bit error probability (BEP):** Gives the probability of making a wrong estimation (in reception) of the information bits that are being applied (in transmission).

4.2.1 Outage Probability

To evaluate the performance of a mobile communication system in practice, it is usually assumed that reception is successful if the instantaneous SNR that is observed in reception (for the given transmission time interval) is good enough, or equivalently, if the received SNR value is above a given threshold. In other words, a certain rate is supported if its instantaneous received SNR satisfies

$$\gamma[i] \geq \gamma_0, \tag{4.29}$$

where the threshold γ_0 is selected to guarantee a certain quality of service (for the given transmission rate). In this situation, the statistical performance measure

$$\Pr\{\gamma[i] \leq \gamma_0\} = \Pr{}_{\text{out}}(\gamma_0) \tag{4.30}$$

is defined as the outage probability of the communication link, for the given target SNR value γ_0. Note that the previously deduced CDF can be used to compute the outage probability of the system in a straightforward way.

4.2.2 Ergodic Capacity

The ergodic capacity [29] is defined as

$$C(\overline{\gamma}) = \mathbb{E}\{\log_2(1+\overline{\gamma}z)\} = \int_0^\infty \log_2(1+\overline{\gamma}z)\, f_Z(z)\, dz, \tag{4.31}$$

where

$$\overline{\gamma} = \frac{P_{\text{tx}}}{P_N} \tag{4.32}$$

is the average SNR, and $f_Z(z)$ is the distribution of Z.

No Channel Feedback

When there is no feedback signaling (i.e., $N = 0$), we see that the PDFs of both, RV $\widetilde{X}_R$ and $\widetilde{X}_I$, follow a Gaussian distribution with zero mean and identical variance (i.e., $\sigma_1 = \sigma_2 = \sigma$), which represent the real and imaginary components of a circularly symmetric complex Gaussian RV. Then, it is possible to conclude that RV Z is exponentially distributed according to

$$f_Z(z) = \beta e^{-\beta z}, \qquad \beta = \frac{1}{2\sigma^2}. \tag{4.33}$$

Using (4.31) and a relation derived in [33], we get

$$C(\overline{\gamma}) \;=\; \log_2(\gamma) + \log_2(e)\left[\exp\left(\frac{1}{2\sigma^2\overline{\gamma}}\right) E_1\left(\frac{1}{2\sigma^2\overline{\gamma}}\right) - \log_e(\overline{\gamma})\right], \tag{4.34}$$

where

$$E_1(z) = \int_z^\infty \frac{e^{-t}}{t}\, dt \tag{4.35}$$

is the exponential integral function of the first order [30].

Limited Channel Feedback

In presence of limited feedback (i.e., when $N \geq 1$), the previous analysis does not hold anymore. When using the PDF derived in (4.23) with $n = 1$, the ergodic capacity attains the form

$$C(\overline{\gamma}) = \sum_{k=0}^{\infty} W_k(\sigma_1, \sigma_2) \int_0^\infty \log_2\left(1 + \overline{\gamma} z\right) f_k(z)\, dz, \tag{4.36}$$

where the weighting factor $W_k(\sigma_1, \sigma_2)$ is defined in (4.25), and the non-central χ^2 PDF $f_k(z)$ is presented in (4.26). Since the exact computation of (4.36) is not straightforward in this case, well-known Jensen's inequality is used instead. It is known that when a RV is concentrated near its mean, Jensen's bound

$$\mathbb{E}\{g(z)\} \leq g(\mathbb{E}\{z\}) \tag{4.37}$$

becomes particularly accurate [31]. To analyze the degree of variability of RV Z around its mean, we use the fading figure

$$\mathcal{F}_Z = \frac{\mathbb{E}^2\{Z\}}{\mathrm{Var}\{Z\}}, \tag{4.38}$$

where the value of

$$\mathbb{E}\{Z\} = \mathbb{E}\{\widetilde{X}_R^2\} + \mathbb{E}\{\widetilde{X}_I^2\} \tag{4.39}$$

can be obtained in closed form with the aid of (4.21) and (4.22); see reference [33] for more details. It can be seen from Table 4.1 that the values

Table 4.1. Fading figure values of the received SNR in presence of different feedback resolutions (N) and numbers of network element (M).

N	M=10	M=20
0	1.112	1.053
1	12.62	23.18
2	262.0	521.4
3	4475.5	9037.6

of fading figure are always greater than 1, and they tend to grow as M and N increase. The only exception is the case $N = 0$, where no coherent combining gain is possible due to the absence of CSI to carry out the co-phasing procedure in transmission; so, in this particular situation, fading figure parameter takes values close 1 in all cases (and tends asymptotically to the unitary value, since the central limit theorem starts to work in a better way when the number of distributed antennas elements M grows large). It is important to highlight that the case $N = 0$ was analyzed separately, following a different approach with respect to the case where limited channel signaling is available. Therefore, closed-form approximation

$$\begin{aligned} C(\bar{\gamma}) &= \mathbb{E}\left\{\log_2(e)\log_e\left[\bar{\gamma}\left(\frac{1}{\bar{\gamma}}+z\right)\right]\right\} \\ &\approx \log_2(e)\left[\log_e(\gamma)+\log_e\left(\frac{1}{\bar{\gamma}}+\mathbb{E}\{z\}\right)\right] \end{aligned} \tag{4.40}$$

provides a good estimation of the ergodic capacity for feedback methods with $N \geq 1$. Actually, closed-form expression (4.40) provides a strict upper bound for the ergodic capacity, which becomes asymptotically optimal as the channel phase resolution grows (i.e., as $N \to \infty$).

4.2.3 Bit Error Probability

The average bit error probability can be computed using the formula

$$\bar{p_e} = \int_0^\infty P_{mod}\left(\bar{\gamma}z\right) f_Z(z) dz, \tag{4.41}$$

where $f_Z(z)$ is the PDF of the instantaneous SNR, and

$$P_{mod}\left(\bar{\gamma}z\right) = Q\left(\sqrt{2\bar{\gamma}z}\right) = \frac{1}{2}\mathbf{erfc}\left(\sqrt{\bar{\gamma}z}\right) \tag{4.42}$$

is the error rate when the modulation scheme is BPSK.
When $f_Z(z)$ is non-central χ^2 distributed, the average BEP can be written

as

$$\begin{aligned} p_e(M) &= p_e(M-1) - \frac{1}{2}\binom{2M-2}{M-1}\sqrt{\frac{d}{1+d}} \\ &\times \left[\frac{1}{4(1+d)}\right]^{M-1} \exp\left[-\frac{\kappa d}{1+d}\right] \\ &\times K\left(\frac{1}{2}, M; -\frac{\kappa}{1+d}\right) \quad M > 1, \end{aligned} \tag{4.43}$$

where $M = \frac{n}{2}$ is the number of channels,

$$\kappa = \frac{s^2}{2\sigma^2} \tag{4.44}$$

is the ratio between the energy of the deterministic component and the average received energy via the random component,

$$d = \sigma^2 \bar{\gamma}, \tag{4.45}$$

and

$$K(a, c; z) = \sum_{n=0}^{\infty} \frac{(a)_n}{(c)_n} \frac{z^n}{n!} \tag{4.46}$$

is the confluent hypergeometric function, where

$$(b)_n = \frac{\Gamma(b+n)}{\Gamma(b)} \tag{4.47}$$

is the so-called Pochhammer's symbol (also known as rising factorial) [30]. When $M = 1$, the error rate is given by

$$p_e(1) = Q(u, w) - \frac{1}{2}\left[1 + \sqrt{\frac{d}{1+d}}\right] \exp\left(-\frac{u^2+w^2}{2}\right) \mathcal{I}_0(uw), \tag{4.48}$$

where

$$u = \sqrt{\frac{\kappa\left[1 + 2d - 2\sqrt{d(1+d)}\right]}{2(1+d)}}, \quad w = \sqrt{\frac{\kappa\left[1 + 2d + 2\sqrt{d(1+d)}\right]}{2(1+d)}}. \tag{4.49}$$

For more details, see [34].

Finally, the BEP that corresponds to the sum of a central and a non-central χ^2 distribution can be expressed by weighted BEP expressions for non-central χ^2 distribution, i.e.,

$$P_e = \sum_{k=0}^{\infty} W_k(\sigma_1, \sigma_2) P_e(k+1), \tag{4.50}$$

where $P_e(k+1)$ is obtained from (4.43)-(4.49), while the weighting factor $W_k(\sigma_1, \sigma_2)$ is given in (4.25).

5. Numerical Results

In this chapter, we study the performance of the dedicated feedback DBF algorithm based on the theoretical framework presented in Chapter 4. We investigate the corresponding outage probability, ergodic capacity, and bit error probability for different amounts of channel phase signaling, for different channel amplitude models (dependent on the physical location of the cooperative network elements), and for various numbers of active RSs. The numerical results for the feedback schemes presented here are based on the results that are available in Publications I and II.

5.1 Performance of Dedicated Feedback Channel Scheme

Regarding the channel amplitude models, we assume that in all cases the total transmission power over all array elements is unitary (i.e., $P_{\mathrm{tx}} = 1$), and that signal gains $\sqrt{\gamma_m}$ are fixed over the whole duration of the data communication. In addition, in those cases where the array elements are grouped in two different clusters (with exactly half the number of active array elements in each one), we use notation

$$\delta = \frac{\overline{\gamma}_{(1)}}{\overline{\gamma}_{(2)}} \tag{5.1}$$

to represents the power imbalance situation between both groups. Here, $\overline{\gamma}_{(1)}$ and $\overline{\gamma}_{(2)}$ represent the individual mean SNRs of the active array elements in the first cluster (stronger channel gains) and the second cluster (weaker channel gains), respectively. The following models for the channel amplitudes are used:

- Amplitudes are random but fixed samples from i.i.d. Rayleigh statistics,

- Amplitudes admit perfect power balance (i.e., $\delta = 0$ dB),

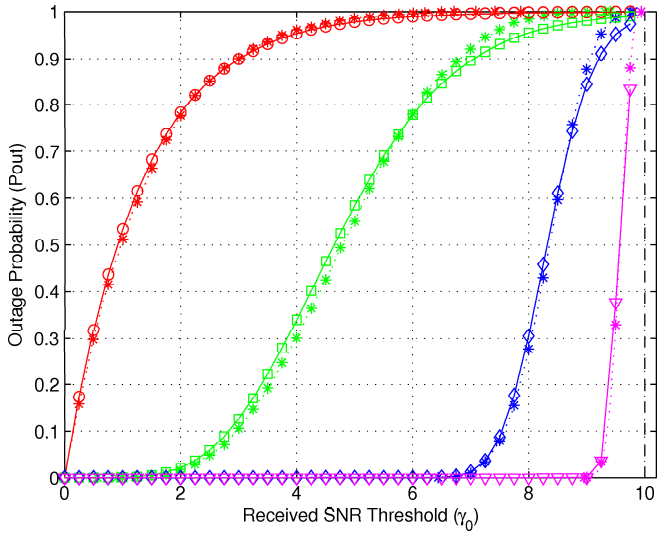

Figure 5.1. Outage probability as a function of SNR threshold γ_0 for DBF with 10 array elements. Solid curves: No CSI ('$\circ$'), $N = 1$ ('$\square$'), $N = 2$ ('$\diamond$'), $N = 3$ ('∇'). Dashed-dotted line: Full CSI at array elements. Simulated values denoted by ('*'). Channel amplitudes are random but fixed samples from Rayleigh statistics.

- Amplitudes experience medium channel power imbalance (i.e., $\delta = 3$ dB), and

- Amplitudes have high channel power imbalance (i.e., $\delta = 6$ dB).

When channel amplitudes are Rayleigh distributed, it is assumed that related random variables are i.i.d. with unitary mean value.

5.1.1 Outage Probability

Fig. 5.1 and Fig. 5.2 show the outage probability for a given SNR threshold, when using the proposed DBF algorithm for different amounts of channel phase signaling in presence of $M = 10$ and $M = 20$ active array elements. Constant Rayleigh distributed channel amplitudes were used to model the amplitudes in this scenario. The solid curves are plotted based on approximation (4.27) with appropriate fitting parameters, along with upper bounds related to the case of full CSI at array elements (dashed line) [1]. In all cases, simulated point values ('$*$') are also included to verify the validation of the analytical results. According to these results, we see that the proposed approximation follows simulated values well. As

[1] Full CSI is here used as a synonym for perfect channel phase information because no channel amplitude information is considered in this Thesis.

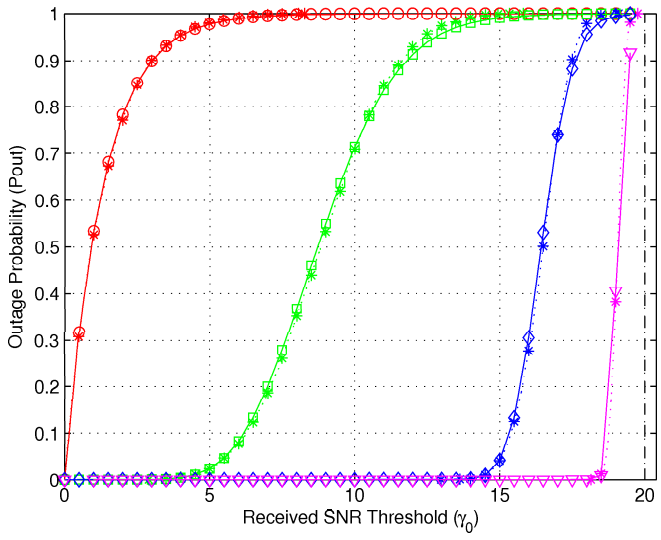

Figure 5.2. Outage probability as a function of SNR threshold γ_0 for DBF with 20 array elements. Solid curves: No CSI ('$\circ$'), $N = 1$ ('$\square$'), $N = 2$ ('$\diamond$'), $N = 3$ ('∇'). Dashed-dotted line: Full CSI at array elements. Simulated values denoted by ('*'). Channel amplitudes are random but fixed samples from Rayleigh statistics.

expected, the accuracy of the approximation is better when the number of active array elements in the system is higher. In Fig. 5.1, the outage probability in absence of channel phase signaling is used as a baseline. It is found that performance in terms of outage probability clearly increases with additional phase bits in the feedback link. We also note that if $N = 3$, then the performance of DBF algorithm is very close to the one observed with full CSI at the elements of the distributed antenna array.

Fig. 5.3 shows the outage probability for a given SNR threshold, when implementing DBF algorithm for different channel power imbalance situations, in presence of $M = 10$ active array elements. In this case, array elements are grouped in two clusters (of the same size), that are located at different distances from the main receiver. Note that mean received SNR values for different antenna elements were selected to guarantee the same performance for different channel power imbalance situations, in absence of signaling information (this is the reason why the different performance curves overlap for the different channel power imbalance situations when $N = 0$). Solid curves, dashed curves, and dotted curves represent perfect channel power balance (i.e., $\delta = 0$ dB), medium channel power imbalance (i.e., $\delta = 3$ dB), and high channel power imbalance (i.e., $\delta = 6$ dB) situations, respectively. Based on the results we observe that, the power imbalance level in the channel amplitude model increases

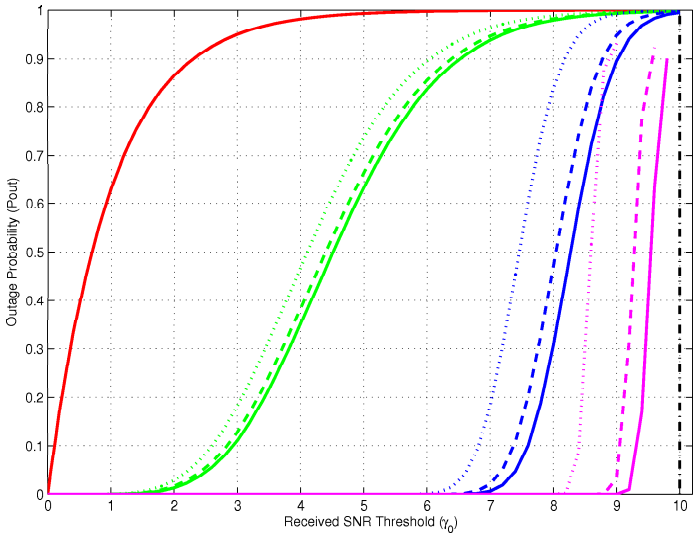

Figure 5.3. Outage probability as a function of SNR threshold γ_0 for DBF with 10 array elements. Solid curves: Perfect channel power balance (i.e., $\delta = 0$ dB). Dashed lines: Medium channel power imbalance (i.e., $\delta = 3$ dB). Dotted curves: Large channel power imbalance (i.e., $\delta = 6$ dB). Channel feedback: No CSI (red), $N = 1$ (green), $N = 2$ (blue), $N = 3$ (magenta). Dashed-dotted line (black): Full CSI at array elements. Channel amplitudes are fixed according to the different channel power imbalance situations.

the outage probability of the DBF algorithm. The larger is the number of phase bits N, the smaller is this impairment. The same behavior is visible when the number of active array elements increases (these figures are not included since those results are similar to the ones that are observed in Fig. 5.3). As expected, in presence of individual channel gains with different average path loss characteristics (i.e., with different long-term signal strength), the variability of the received SNR increases at the main receiver, causing a less abrupt improvement in the sigmoid function of the CDF as the value of γ_0 grows.

Finally, Fig. 5.4 presents the maximum SNR threshold that can be guaranteed for a given outage probability when implementing the proposed DBF algorithm in a perfect channel power balance case (i.e., when $\delta = 0$ dB). These curves admit almost linear behavior with respect to the number of active array elements. Based on these curves we observe that, as N grows, the gap between the different outage probability curves decreases. This is in accordance with the behavior of the expected value of the real part of the sum channel (i.e., μ_R), given in equation (4.20) and presented in Fig. 5.5.

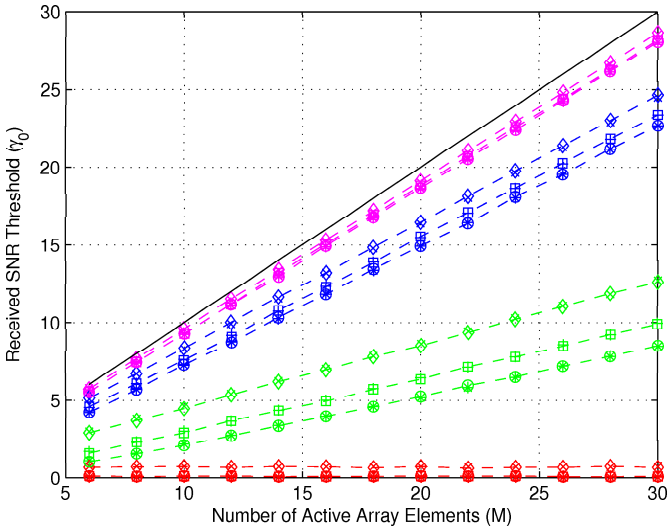

Figure 5.4. Required SNR threshold γ_0 for DBF to guarantee a given outage probability as a function of number active array elements. Outage probability: $\Pr_{\text{out}} = 0.02$ ('$\circ$'), $\Pr_{\text{out}} = 0.1$ ('$\square$'), $\Pr_{\text{out}} = 0.5$ ('$\diamondsuit$'). Channel feedback: No CSI (red), $N = 1$ (green), $N = 2$ (blue), $N = 3$ (magenta). Solid line: Full CSI at array elements. Simulated values denoted by ('*'). Channel amplitudes are fixed with perfect power balance.

5.1.2 Ergodic Capacity

Figures 5.6-5.7 show the ergodic capacity as a function of the number of active array elements (i.e., M) and phase feedback bits per network element (i.e., N), respectively. A set of (constant) Rayleigh i.i.d. samples were used to model the individual channel amplitudes in the second hop. In the case of limited channel phase signaling, the curves were plotted based on the approximation (4.37). In absence of channel phase signaling (i.e., for $N = 0$), the closed-form expression (4.34) was used. Simulated point values ('$*$') are also included to verify the accuracy of the approximation, which was proposed to estimate the values of the ergodic capacity in the different situations. Note that as expected, the ergodic capacity performance increases when both, the resolution of the channel phase information and the number of cooperative network elements grow. The solid curve in Fig. 5.6 represents asymptotic upper bound with full CSI at the RSs. Note that the proposed approximation provides results very close to the theoretical upper bound, when the channel phase resolution $N = 3$ bits/RS.

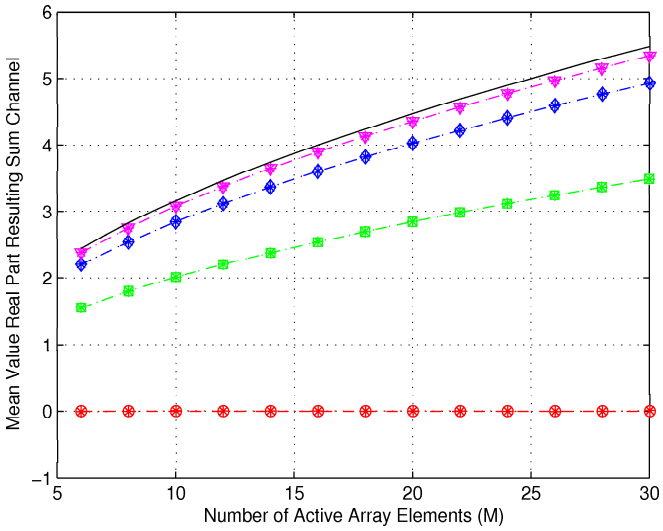

Figure 5.5. Expected value for the real part of the sum channel μ_R as a function of number active array elements. Dashed curves: No CSI ('○'), $N = 1$ ('□'), $N = 2$ ('◇'), $N = 3$ ('▽'). Solid line: Full CSI at array elements. Simulated values denoted by ('*'). Channel amplitudes are fixed with perfect power balance.

5.1.3 Bit Error Probability

Fig. 5.8 presents the BEP curves that are achieved when implemented our DBF algorithm with different amounts of channel phase signaling in the second hop. Dashed and dotted lines represent the theoretical and simulated results, respectively. Solid line represents the BEP lower bound situation, achieved when using BPSK modulation in an equivalent AWGN channel model. According to these results, it is possible to conclude that, the proposed theoretical model approximates the simulated results of our DBF algorithm in an accurate way. It is also straightforward to see that, when the number of phase bits exceeds $N = 2$ bits/RS, the proposed approximated methods provide a BEP curve that is very close to the one that corresponds to an equivalent AWGN channel model (i.e., lower bound for our BEP analysis). Note that these simulation results support the previously presented claim (for both, outage probability and ergodic capacity analyses), that the use of channel phase resolution exceeding $N = 3$ bits/RS does not provide additional improvements in the end-to-end performance of our cooperative system model.

In the light of all results we see that there is no reason to use more than $N = 3$ bits/RS to implement a DBF algorithm in the second hop of our cooperative wireless scenario. Yet, the performance that is obtained with

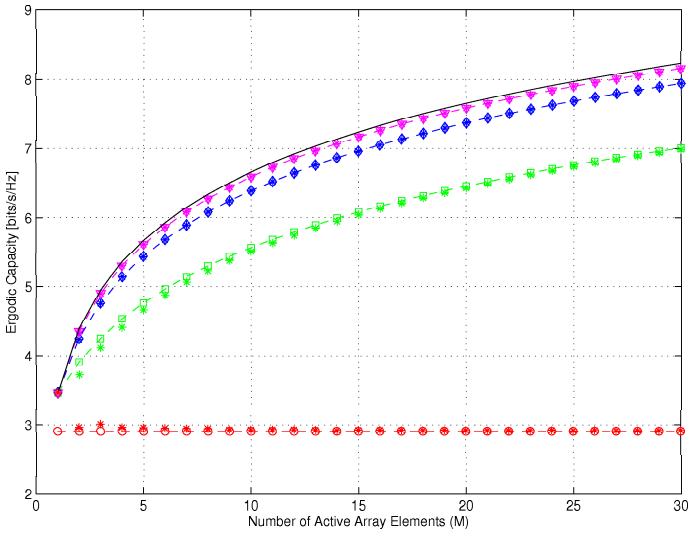

Figure 5.6. Ergodic capacities with different number of phase bits as a function of number of active array elements, when the average SNR $\overline{\gamma} = 10$[dB]. The dashed lines represent the theoretical curves: $N = 0$ ('$\circ$'), $N = 1$ ('$\square$'), $N = 2$ ('$\diamond$'), $N = 3$ ('$\triangledown$'). Solid line: Full CSI at RSs. Simulated values denoted by ('*'). Channel amplitudes are fixed with perfect power balance.

$N = 1$ bit/RS is not good enough. However, the performance obtained with $N = 2$ bits/RS provides a reasonable trade-off between *the cost* of signaling overhead, and *the benefit* that the improvement in the different performance measures under analysis (i.e., outage probability, ergodic capacity, and bit error probability) represent.

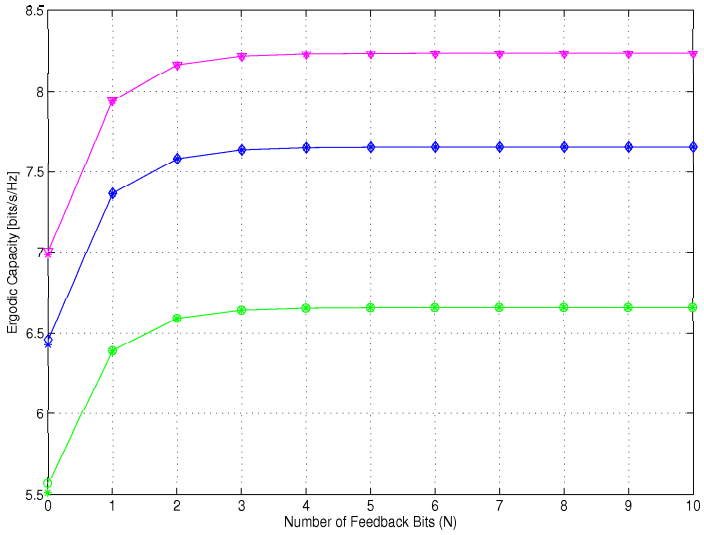

Figure 5.7. Ergodic capacities with different number of active array elements as a function of number of phase bits, when the average SNR $\overline{\gamma} = 10\,[\mathrm{dB}]$. The solid lines represent the theoretical curves: $M = 10$ ('□'), $M = 20$ ('◇'), $M = 30$ ('▽'). Simulated values denoted by ('*'). Channel amplitudes are fixed with perfect power balance.

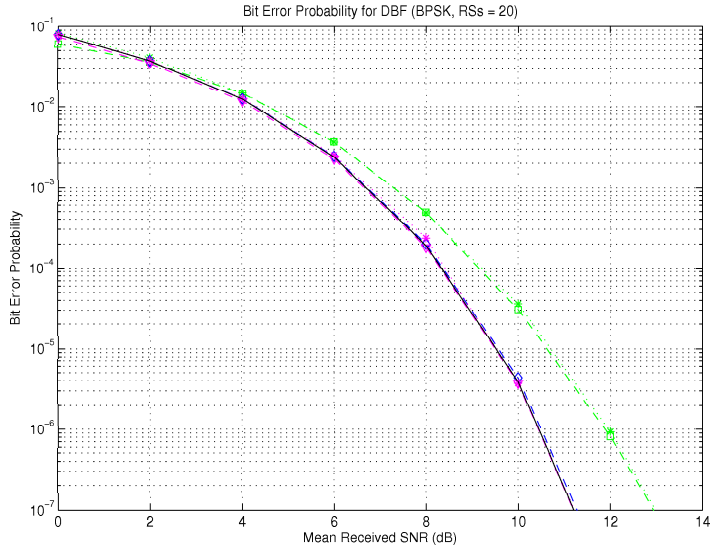

Figure 5.8. Bit error probabilities with different number of phase bits, when the number of active array elements $M = 20$. Dashed lines represent the theoretical models: $N = 1$ ('□'), $N = 2$ ('◇'), $N = 3$ ('▽'). Dotted lines represents the corresponding simulated models ('$*$'). Solid line represents the AWGN channel lower bound. Channel amplitudes are fixed with perfect power balance.

6. Common Feedback Approach

Whereas the main focus of this Thesis was set on the methods with an individual feedback channel, in this chapter, the system with a common feedback channel is briefly studied. The concept was introduced by Mudumbai et al. in [35], and the following extending research is based on recent unpublished research made between the publications I and II by the author of this Thesis, its instructor, and the supervisor. The performance of the common feedback DBF scheme is not studied in detail in this Thesis, but a number of improvements over the original idea by Mudumbai et al. are considered. The suggested improvements are investigated for two cases. When:

1. There is only single transmitter/receiver, and

2. There are two transmitters/receivers.

For the single receiver case, the use of adaptive range for the (random) phase perturbations is compared to the original case with full range perturbations, followed by a comparison in terms of different number of active RSs. Then, the different selection criteria (to decide whether to update the phases or not) are compared in the multi receiver case.
The behaviour of the common feedback scheme introduced by Mudumbai et al. resembles a random walk (RW) and therefore, unlike in the individual feedback channel, treatable theoretical results can be derived solely in the case of full random phase perturbations.

6.1 Differences to the Scheme Presented by Mudumbai

Even though the basic idea is the same, the common feedback scheme used here differs slightly from the one introduced by Mudumbai et al. in [35], where a cluster of energy-constrained wireless sensor nodes utilizing a master-slave architecture are used to communicate with a distant BS. The system model used in this Thesis differs in the part that there is a first hop from a separate transmitter to the array elements. In addition, whereas the environment in [35] was not defined, the main focus here is on the indoor enviroment, where the user is surrounded by large number of low-cost low-power RSs. We note that only the initial results of the suggested improvements to the Mudumbai method are presented.

6.2 Common Feedback Channel

The system model is similar to the one used in case of individual feedback channel in Fig. 3.2, with the exception that the feedback channel is common for all RSs. In the second hop of the communication link there are M active array elements transmitting the same stream of complex symbols to the main receiver. The idea behind the adaptive 1-bit common feedback DBF algorithm by Mudumbai et al. can be summarized as follows:

1. An independent random phase adjustments at each RS in each iteration of the algorithm.

2. Then, the receiver broadcasts 1-bit feedback per iteration to inform whether its aggregate SNR is better or worse than the previous one.

3. Only the phases that increase the aggregate SNR at the main receiver are retained.

The SNR at the main receiver is given by

$$\gamma[n] = \left| \sum_{m=1}^{M} \left(\sqrt{\gamma_m} e^{j\psi_m} \right) w_m[i] \right|^2, \tag{6.1}$$

where ψ_m is a random channel phase response from the m-th array element, and w_m is the beamforming weight. Each RS keeps track of the best know beamforming weight

$$\widetilde{w}_{best,m}[n] = \sqrt{P_{tx}} e^{-j\phi_{best,m}[n]}, \tag{6.2}$$

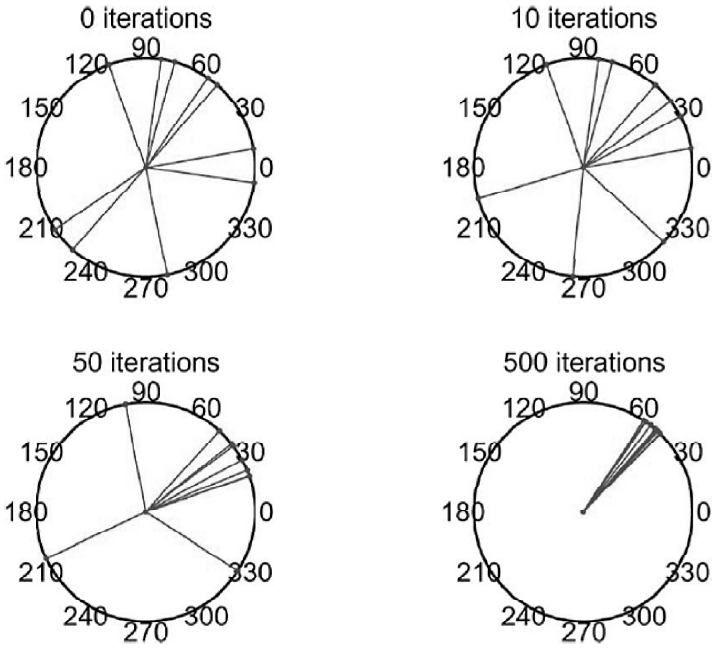

Figure 6.1. Convergence of feedback control algorithm over iterations, when there are $M = 10$ RSs [36].

where $\phi_{best,m}$ is the best know value of the phase rotation. In each iteration a random phase perturbation is added, i.e.,

$$\widetilde{\phi}_m[n+1] = \widetilde{\phi}_{best,m}[n] + \delta_m. \tag{6.3}$$

If the best observed SNR

$$\widetilde{\gamma}_{best}[n] = \mathbf{max}_{i \leq n} \left| \sum_{m=1}^{M} \left(\sqrt{\gamma_m} e^{j\psi_m} \right) \widetilde{w}_m[i] \right|^2 \tag{6.4}$$

is improved, then the $\widetilde{\phi}_m[n+1]$ is stored as the new $\widetilde{\phi}_{best,m}[n]$.
The perturbations δ_m can be either (uniformly) continuous on interval $[-\delta_M, \delta_M]$, or equivalently (uniformly) discrete with (for example) two values at $-\frac{1}{2}\delta_M$ and $-\frac{1}{2}\delta_M$. Fig. 6.1 illustrates the convergence of phases to beamforming with $M = 10$ RSs [36].

6.2.1 Random Walk

The statistical behaviour of (continuous) RV (6.1) resembles Pearson's RW problem. Random walk is a mathematical formalisation of a path that consists of a succession of random steps. The original problem is the following: A man starts from a point O and walks l yards in a straight line; then, he turns through any angle whatever and walks another l yards in a second straight line. He repeats this process n times. What is the probability that after n of these stretches he is at a distance between r and

$r + \delta r$ from his starting point O. In two-dimensional isotropic walk, a step is taken towards a random direction in a two-dimensional grid. The practical difference between the SNR (6.1) and the RW problem is that in the RW case, the distribution is analyzed for the end-to-end distance r after a chain of randomly chosen steps (of equal length), rather than for the sum signal squared as in (6.1). The distribution for the end-to-end distance has been extensively analyzed, but closed-form expressions for the PDF have only been derived for $n = 1, 2, 3$ steps. However, an integral form for the PDF in case of $n \to \infty$, has been derived by Rayleigh.
The mentioned PDF for the end-to-end distance r is

$$f_n(\mathbf{r}) = \frac{1}{2\pi} \int_0^\infty u J_0\left(u|\mathbf{r}|\right) J_0\left(ua\right)^n du, \tag{6.5}$$

where a is the step size, n is the number of steps, and

$$J_\alpha(x) = \frac{i^{-\alpha}}{\pi} \int_0^\pi \cos(\alpha\theta) \exp\left(ix\cos\theta\right) d\theta \tag{6.6}$$

is the α-th order Bessel function of the first kind [30] . The asymptotic solution by Rayleigh for the PDF is based on two-dimensional central limit theorem:

$$f_n(\mathbf{r}) = \frac{1}{\pi n a^2} \exp\left\{-\frac{|\mathbf{r}|^2}{na^2}\right\}. \tag{6.7}$$

Now, since we know the distribution of the length of the RW, we can also calculate the probability that the walker is less than a distance r from the starting point after n steps (i.e. the CDF):

$$F_n(r) = r \int_0^\infty J_1(ur) J_0(ua)^n du. \tag{6.8}$$

There is no closed-form expression for general values of n, but a numerical solution can be derived as follows:

$$F_n(r) = \frac{2r}{r_{max}} \sum_{m=1}^{\infty} \frac{1}{j_m J_1\left(j_m\right)^2} J_1\left(j_m r / r_{max}\right) J_0\left(j_m a / r_{max}\right)^n, \tag{6.9}$$

where

$$r_{max} = na \tag{6.10}$$

is the maximum distance after n steps, and j_m denotes the m-th smallest positive zero of J_0.
In case of discrete phase perturbation, the behaviour of RV (6.1) resembles Polya's RW in two dimensional lattice (for range of $\pi/4$). Unfortunately there is no closed-form expression defined for it, and therefore the observation is of little use [37].

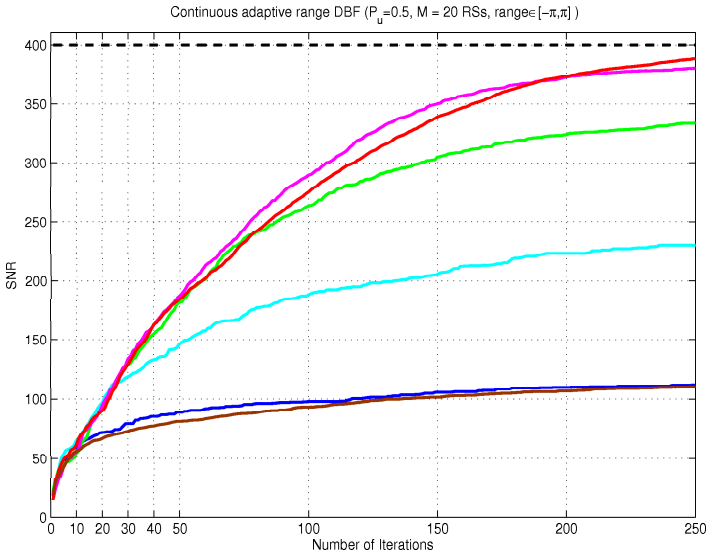

Figure 6.2. The evolution of the received SNR as a function of number of iterations for adaptive range. Blue curve: (Full) range remains constant the whole time. Cyan curve: Range halved once. Green curve: Range halved twice. Magenta curve: Range halved three times. Red curve: Range halved four times. The reductions are done every 10 iterations. Brown curve: Common phase update probability $p_u = 0.5$ (the probability whether to update the phase of an individual RS). Dashed figure represents the upper bound. 20 RSs used.

6.3 Single Receiver

The behaviour of RV (6.1) can be modeled as a RW of Section 6.2.1. So, the theoretical model for the SNR in a single receiver case can be presented accordingly. The best observed SNR (6.4) corresponds to the largest order statistic of I i.i.d. iterations (i.e., a step in the best direction). By using the definition for the expected value, the desired SNR is obtained as follows:

$$\gamma_t = \nu - \int_0^m F_n(r)^I dr, \tag{6.11}$$

where ν is the maximum distance of the random walker squared (maximum distance in this case) [38].

Adaptive Range

To improve the original algorithm, adaptive range perturbations can be used. The range of the random phase perturbations can be decreased after certain number of iterations; i.e., based on the observed best SNR, the area of the random phase rotations can be reduced to increase the efficiency. In Fig. 6.2, the (full) range is halved every 10 iterations. Clearly the adaptive range gives better performance than the static range, and after 3 or 4 reductions the SNR is already very close to the theoretical upper bound.

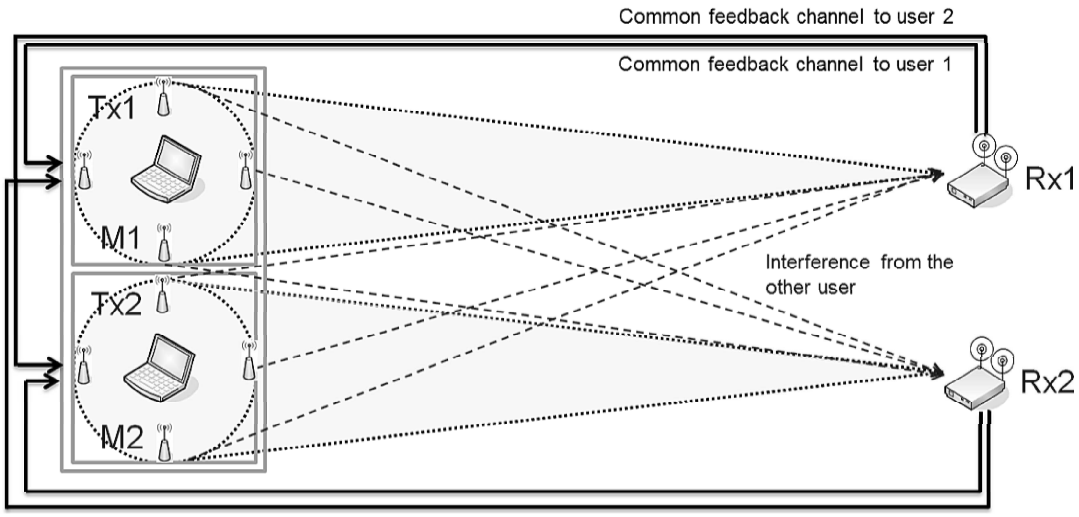

Figure 6.3. The system model for two users in neighbouring rooms, where the users cause interference to each other. There are common feedback channels from both receivers to both RS clusters.

Number of Active Relays

Another possible way to improve the system studied here is to change the phase updating probability of the individual channels. If all the phases are randomly altered after every iteration, whether the resulting aggregate SNR improves, is completely random approach. If the aggregate SNR is improved, all of the phases are updated, whether an individual phase alteration was improving the SNR or not. Since we do not know which phase perturbations were done in the right direction, we can randomly choose which phases get updated and which keep the last best value. After a number of iterations, when the aggregate SNR has improved enough, it would make sense to alter the phases of a smaller group of array elements. A common update probability p_u is given to each array element. However, reducing the update probability resulted in worsened performance, and therefore only the case of $p_u = 0.5$ is included in Fig. 6.2 (the brown curve).

6.4 Multiple Receivers

In case of more than one receivers (two in this case), a different performance criterion is required. Let us consider a situation where there are two separate clusters of RSs and two BSs. They both have different signals and channels and, therefore, naturally cause interference to each other. This system model is presented in the Fig. 6.3. Let us first define

the the SINR in the first receiver as follows:

$$\mathrm{SINR}_1[i] = \frac{\left|\sum_{m=1}^{M_1}\left(\sqrt{\gamma_{11,m}}e^{j\psi_{11,m}}\right)\widetilde{w}_{1,m}[i]\right|^2}{\left|\sum_{n=1}^{M_2}\left(\sqrt{\gamma_{21,n}}e^{j\psi_{21,n}}\right)\widetilde{w}_{2,n}[i]\right|^2 + N_0}, \tag{6.12}$$

where $\{\gamma_{ij,m}\}_{m=1}^{M_i}$ are the individual channel SNRs from user i to user j, M_i is the number of RSs in a cluster for user i, $\{\psi_{ij,m}\}_{m=1}^{M_i}$ are the individual random phases of the channels from user i to user j, $\widetilde{w}_{i,m}$ is the beamforming weight applied by the user i, and N_0 is the noise power. The numerator is the SNR of the first user, and the denominator contains the interference caused by the other user and noise. Similarly, the SINR in the second receiver is

$$\mathrm{SINR}_2[i] = \frac{\left|\sum_{m=1}^{M_2}\left(\sqrt{\gamma_{22,m}}e^{j\psi_{22,m}}\right)\widetilde{w}_{2,m}[i]\right|^2}{\left|\sum_{n=1}^{M_1}\left(\sqrt{\gamma_{12,n}}e^{j\psi_{12,n}}\right)\widetilde{w}_{1,n}[i]\right|^2 + N_0}. \tag{6.13}$$

The aim is to maximize the sum-rate of the users, i.e.,

$$R_{sum} = \log_2(1+\mathrm{SINR}_1) + \log_2(1+\mathrm{SINR}_2). \tag{6.14}$$

Since the transmitters do not know the sum-rate, but only whether the SINRs are improved or not, deciding whether to update the beamforming weights is more challenging than in the single receiver case. It is clear that if both receivers report an improvement in SINR, the beamforming weights are updated. If both report a decrease in the SINR, the beamforming weights are not updated. But when one receiver informs about improvement, but the other does not, a problem arises whether to update or not. In this Thesis three options are considered:

1. The systems are considered separate systems, and the decisions are based on the SNR like in the single receiver case (i.e., ignore the other user and update when own SNR is improved).

2. Decisions are based on the SINR, taking account the interference from the other user (i.e., update only when both SINR values are improved).

3. Decisions are based on the interference caused by the interfering system (i.e., update when the interferences to each other are reduced).

If we assume that the interference caused by the other user can be differentiated from the received signal (e.g., using orthogonal pilot signals in

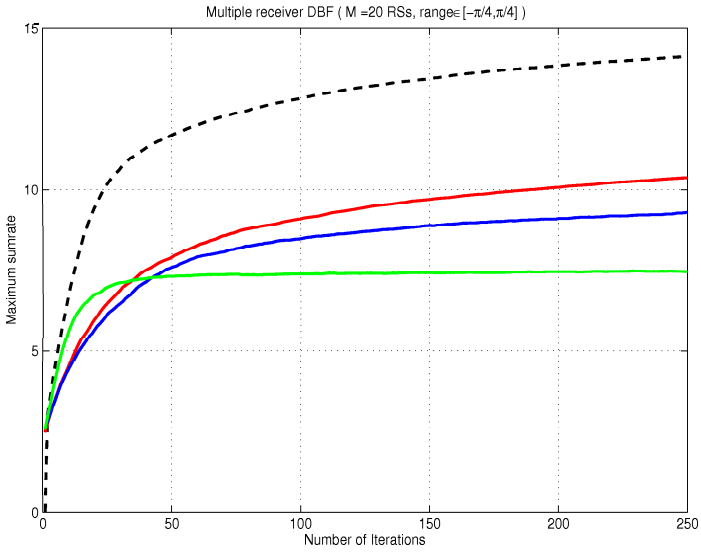

Figure 6.4. A comparison between the different decision making choises for achieving the best sum-rate. Red curve: Beamforming weights updated only when both SINRs improved. Blue curve: Systems considered separately. Green curve: Interference based decision. Dashed line: Simulated upper bound approximation.

different clusters), the decision whether to update the phase can be made based on the interference level caused by the other user; i.e., the denominators in (6.12) and (6.13). When the interference in one receiver decreases, the receiver suggests the interfering user to update the weights. To the best knowledge of the author, unlike the single receiver case, there is no simple way of calculating the theoretical formula for the common feedback scheme when there are multiple receivers. Therefore, no closed-form formula is presented here.

The comparison between the three criteria are shown in Fig. 6.4. The interference based method starts out best, but performance saturates fast. This is due to decision making not being about improving the sum-rate, but rather keeping the interference as low as possible whether it improves the SINR or not. As expected, the SINR based criterion performs better than the SNR based criterion. Therefore, out of the three criteria considered here, the SINR based criterion performs the best in the long run. The upper bound is approximated by setting the interferences to zero and, therefore, its performance is better than what could be achieved in reality.

7. Conclusions

7.1 Summary of Conclusions

The goal of this Thesis was to study the new distributed beamforming (DBF) techniques, to mitigate the effect of losses present in an indoor enviroment. The proposed idea was to boost the performance of an indoor subscriber (main transmitter) by utilizing a massive cluster of cooperative network elements that are located in close proximity. The cooperative network is composed by fixed low-cost array elements, which could be located for example in the walls and ceiling of a room. The massive deployment of inexpensive array elements enables the implementation of a DBF scheme, where the beamforming weights are updated by a limited feedback scheme. Two feedback channel models were presented: dedicated feedback channel and common feedback channel models. The main focus was put on the dedicated feedback channel.

To validate the feedback channel scheme, the performance of a DBF algorithm in presence of different amounts of channel phase feedback information was studied. Due to short distances, the communication over the first hop (i.e., from main transmitter to elements of the distributed array) was assumed to be costless in terms of transmission power and radio resource usage. Therefore, the bottleneck of the system model was assumed to be located in the second hop (i.e., from the elements of the disperse antenna array to the main receiver).

Three different performance measures were used to study the performance of the DBF algorithm: outage capacity, ergodic capacity, and bit error probability. To carry out the analysis, suitable closed-form approximations for *probability distribution function* (PDF) and *cumulative distribution function* (CDF) of received *signal-to-noise* power *ratio* (SNR) were

derived. The parameters for the approximations were obtained from the first two raw moments of the resulting sum channel that the main receiver observes. With the aid of these PDF and CDF expressions, useful closed-form formulas for the selected performance parameters were derived. All these approximations were validated using numerical simulations. The analysis revealed that notable gains can be achieved in terms of all different performance measures, when using a small amount of phase feedback information in the DBF algorithm that is configured in the second hop of our cooperative system scenario.

In addition, several ways to improve the common feedback channel scheme were considered. For the single receiver case the use of adaptive phase perturbations resulted in considerably better performance, whereas the use of varying number of active relay stations (RSs) resulted in slightly worsened performance. In case of multiple receivers different selection criteria for updating the phase were investigated. The SNR and interference based criteria resulted in worse performance than the *signal-to-interference-plus-noise* power *ratio* (SINR) based criterion.

7.2 Future Work

Before finishing this Thesis, we present a possible future extension to the studied schemes. Apart from the power saving capabilities that a cooperative cluster of RSs provides to a mobile station (MS), the implementation of a DBF scheme (aided by RSs) has many potential applications in the context of future *heterogeneous networks* (HetNets). As heterogeneous networks are composed by a mixture of different kind of network elements, where a large number of low-power *femto base stations* (FBSs) is expected to coexist in the same geographical location, with high-power *macro base stations* (MBSs), severe interference problems occur in the network, which create special challenge due to the following facts:

- Unplanned deployments of FBSs and well-planned deployments of MBSs are expected to coexist in the same frequency bands, generating co-channel interference.

- Closed-subscriber configuration is expected to be used at many FBS deployments, creating strong interference to those MSs that are not identified as members of the group (no handovers are allowed towards FBS

in this situation).

- Large power differences between different network elements will increase the likelihood of having strong interference situations, putting more stringent requirements in the design of interference mitigation schemes for HetNets deployments.

The use of antenna arrays allows to control the interference problem in the different nodes of the HetNet, due to the possibility of reaping beamforming gain in the link between MS and the desired BS. No beamforming gain can be obtained in the interference links, because beamforming weights do not depend on the channel gains of the cross links. As a consequence, the received SINR will be increased by a factor that is proportional to the number of network elements that implement DBF in the second hop.

Two simple illustrative cases are shown in Figs. 7.1-7.2, for the more detailed analysis in future:

1. **Cross-layer interference:** When the cluster of RSs implement a DBF in the uplink direction of the macrocellular link, it can also enable the mitigation of the cross-layer interference that the neighboring FBS is observing in uplink. The opposite situation will take place if MS tries to reach the distant MBS directly, without exploiting the potential beamforming gain that the cluster of RSs provides (see Fig. 7.1).

2. **Co-layer interference:** In this situation, the usage of DBF enables the coexistence of two closed-access FBSs that share the same geographical location (e.g., the same office building), focusing the uplink power of MS in the spatial direction of the intended FBS (see Fig. 7.2). Note that the absence of a RS cluster renders high-rate communication impossible in this scenario, since severe co-channel interference will be generated if MS tries to reach the intended FBS in one hop.

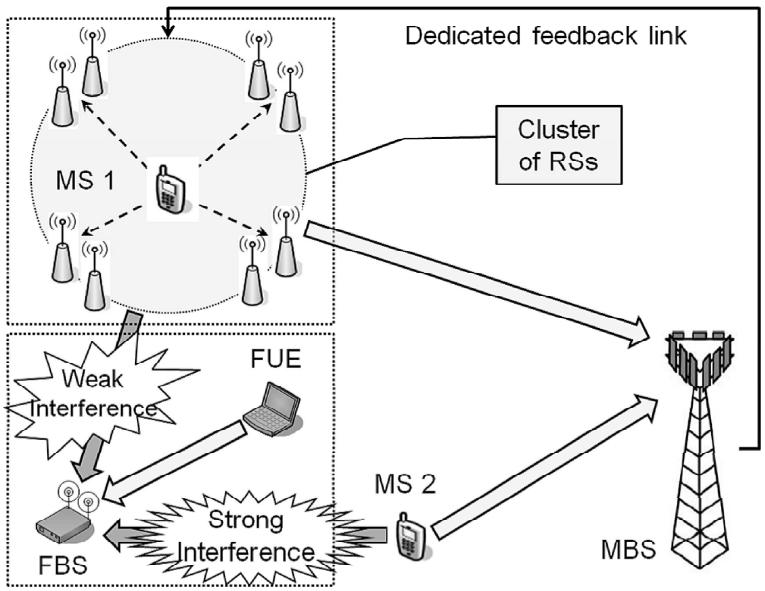

Figure 7.1. Distributed beamforming to mitigate cross-layer interference in a HetNet. The usage of a cluster of relay stations (RSs) reduces that uplink co-channel interference that the mobile station (MS) 1 generates to the neighboring femto base station (FBS). The opposite situation takes place with the uplink co-channel interference that MS 2 generates to the FBS.

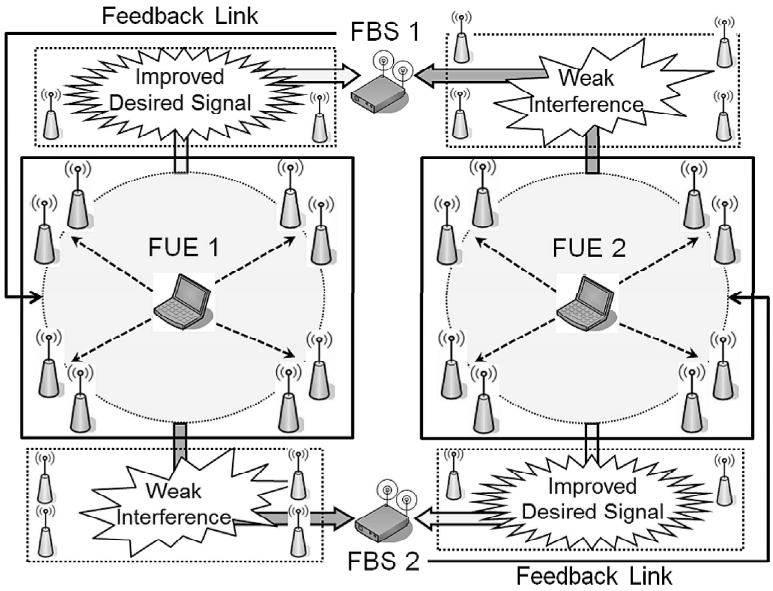

Figure 7.2. Distributed beamforming to mitigate co-layer interference in a HetNet. The usage of a cluster of RSs allows the uplink coexistence of two co-located FBSs that give coverage in the same office building. The uplink interference that would be generated if MS tries to reach the intended FBS in one hop would limit the effective data rate of the system considerably, due to severe co-channel interference.

Bibliography

[1] ITU, "Assessment of the global mobile broadband deployments and forecasts for international mobile telecommunications," *Report ITU-R M.2243 (00/2011)*, pp. 1–96, Nov. 2011.

[2] Ericcson, "More than 50 billion connected devices," *white paper*, pp. 1–12, Feb. 2011.

[3] S. Liu, J. Wu, C. H. Koh, and V. Lau, "A 25 gb/s(/km^2) urban wireless network beyond imt-advanced," *IEEE Commun. Mag.*, vol. 49, no. 2, pp. 122–129, Feb. 2011.

[4] V. Chandrasekhar, J. Andrews, and A. Gatherer, "Femtocell networks: a survey," *IEEE Commun. Mag.*, vol. 46, no. 9, pp. 59–67, Sep. 2008.

[5] M. Kuhn, S. Berger, I. Hammerstom, and A. Wittneben, "Power line enhanced cooperative wireless communications," *IEEE J. Sel. Areas Commun.*, vol. 24, no. 7, pp. 1401–1410, Jul. 2006.

[6] H. Li, J. Hajipour, A. Attar, and V. C. M. Leung, "Efficient hetnet implementation using broadband wireless access with fiber-connected massively distributed antennas architecture," *IEEE Commun. Mag.*, vol. 18, no. 3, pp. 72–78, Jun. 2011.

[7] G. Mansfield, "Femtocells in the US market–business drivers and consumer propositions," in *FemtoCells Europe*. AT&T, London, U.K., Jun. 2008.

[8] R. Pabst, B. Walke, D. Schultz, P. Herhold, H. Yanikomeroglu, S. Mukherjee, *et al.*, "Relay-based deployment concepts for wireless and mobile broadband radio," *IEEE Commun. Mag.*, vol. 42, no. 9, pp. 80–89, Sep. 2004.

[9] M. Husso, J. Hämäläinen, R. Jänti, J. Li, E. Mutafungwa, R. Wichman, *et al.*, "Interference mitigation by practical transmit beamforming methods in closed femtocells," *EURASIP Journal on Wireless Communications and Networking*, vol. 2010, pp. 1–12, Apr. 2010.

[10] R. Mudumbai, D. Brown, U. Madhow, and H. Poor, "Distributed transmit beamforming: challenges and recent progress," *IEEE Commun. Mag.*, vol. 47, no. 2, pp. 102–110, Feb. 2009.

[11] M. Dohler and Y. Li, *Cooperative Communications -Hardware, Channel & PHY*. Wiley, 2010.

[12] X.-H. You, D.-M. Wang, B. Sheng, X.-Q. Gao, X.-S. Zhao, and M. Chen, "Cooperative distributed antenna systems for mobile communications," *IEEE Wireless Commun. Mag.*, vol. 17, no. 3, pp. 35–43, Jun. 2010.

[13] A. B. Saleh, S. Redana, B. Raaf, T. Riihonen, J. Hämälainen, and R. Wichman, "Performance of amplify-and-forward and decode-and-forward relays in lte-advanced," *Proc. IEEE. Vehicular Technology Conference Fall (VTC 2009-Fall)*, pp. 1–5, 2009.

[14] M. Sauer, A. Kobyakov, and J. George, "Radio over fiber for picocellular network architectures," *IEEE. J. Lightwave Tech.*, vol. 25, no. 11, pp. 3302–3320, Nov. 2007.

[15] A. Goldsmith, *Wireless Communications*. Cambridge University Press, 2005.

[16] L. Zheng and D. N. C. Tse, "Diversity and multiplexing: A fundamental tradeoff in multiple-antenna channels," *IEEE Trans. Inf. Theory*, vol. 49, no. 5, pp. 1073–1096, May 2003.

[17] A. J. Paulraj, D. A. Gore, R. U. Nabar, and H. Bölcskei, "An overview of MIMO communications - a key to gigabit wireless," *Proc. IEEE*, pp. 198–218, 2004.

[18] B. Van Veen, "Beamforming: a versatile approach to spatial filtering," *IEEE. ASSP Mag.*, vol. 5, no. 2, pp. 4–24, Apr. 1988.

[19] B. Wardrop, "Digital beamforming and adaptive techniques," *IEE Tutorial Meeting on Phased Array Radar*, pp. 3/1–328, Sep. 1989.

[20] R. Gaokar and A. Cheeran, "Performance analysis of beamforming algorithms," *International Journal of Electronic & Communication Technology*, vol. 2, no. 1, pp. 43–48, Mar. 2011.

[21] D. Tse and P. Viswanath, *Fundamentals of Wireless Communication*. Cambridge University Press, 2005.

[22] H. Hu, Y. Zhang, and J. Luo, *Distributed Antenna Systems: Open Architecture for Future Wireless Communications*. Auerbach Publications, 2007.

[23] A. Saleh, A. Rustako, and R. Roman, "Distributed antennas for indoor radio communications," *IEEE Trans. Commun.*, vol. 35, no. 12, pp. 1245–1251, Dec. 1987.

[24] T. Alade, H. Zhu, and H. Osman, "Performance evaluation of in-building DAS for high data rate wireless transmission," *Proc. IEEE. Wireless Communications and Networking Conference (WCNC)*, pp. 759–764, 2012.

[25] Z. Ding, W. H. Chin, and K. Leung, "Distributed beamforming and power allocation for cooperative networks," *IEEE Trans. Wireless Commun.*, vol. 7, no. 5, pp. 1817 –1822, May 2008.

[26] X. Chen, S. Song, and K. Letaief, "Transmit and cooperative beamforming in multi-relay systems," in *Proc. IEEE Int. Conf. on Commun.*, May 2010, pp. 1 –5.

[27] J. Litva and T. K. Lo, *Digital Beamforming In Wireless Communications*, 1st ed. Artech House Publishers, 1996.

[28] J. Hämäläinen, R. Wichman, A. A. Dowhuszko, and G. Corral-Briones, "Capacity of generalized UTRA FDD closed-loop transmit diversity modes," *Wireless Personal Communications*, vol. 54, no. 3, pp. 467–484, 2010.

[29] J. G. Proakis, *Digital Communications*, 4th ed. McGraw-Hill International Editions, 2001.

[30] M. Abramowitz and I. A. Stegun, *Handbook of mathematical functions: with formulas, graphs, and mathematical tables*. Dover Publications, 1970.

[31] A. Papoulis, *Probability, Random Variables, and Stochastic Processes*, 3rd ed. McGraw-Hill International Editions, 1991.

[32] E. Biglieri, J. Proakis, and S. Shamai, "Fading channels: information-theoretic and communications aspects," *IEEE Trans. Inf. Theory*, vol. 44, no. 6, pp. 2619 –2692, Oct. 1998.

[33] A. A. Dowhuszko, G. Corral-Briones, J. Hämäläinen, and R. Wichman, "On throughput-fairness tradeoff in virtual MIMO systems with limited feedback," *EURASIP Journal on Wireless Communications and Networking*, vol. 2009, pp. 1–17, Jan. 2009.

[34] W. C. Lindsey, "Error probabilities for rician fading multichannel reception of binary and n-ary signals," *IEEE Trans. Inf. Theory*, vol. 10, no. 4, pp. 339–350, 1964.

[35] R. Mudumbai, G. Barriac, and U. Madhow, "On the feasibility of distributed beamforming in wireless networks," *IEEE Trans. Wireless Commun.*, vol. 6, no. 5, pp. 1754 –1763, May 2007.

[36] R. Mudumbai, J. Hespanha, U. Madhow, and G. Barriac, "Distributed transmit beamforming using feedback control," *IEEE Trans. Inf. Theory*, vol. 56, no. 1, pp. 411–426, Jan. 2010.

[37] B. B. Hughes, *Random Walks and Random Environments, Vol. 1: Random Walks*. Oxford University Press, Mar. 1995.

[38] C. K. Au-Yeung and D. J. Love, "On the performance of random vector quantization limited feedback beamforming in a MISO system," *IEEE Trans. Wireless Commun.*, vol. 6, no. 2, pp. 458–462, Feb. 2007.

Publication I

Turo Halinen, Alexis A. Dowhuszko, and Jyri Hämäläinen. Performance of Distributed Beamforming for Dense Relay Deployments in Presence of Limited Feedback Information. *Submitted to EURASIP Journal on Advances in Signal Processing Special Issue on "Advanced Distributed Wireless Communication Techniques - Theory and Practice"*, Jun. 2012.

Publication II

Alexis A. Dowhuszko, Turo Halinen, Jyri Hämäläinen, and Olav Tirkkonen. Performance of Relay-Aided Distributed Beamforming Techniques in Presence of Limited Feedback Information. In *Conference on Performance, Safety and Robustness in Complex Systems and Applications 2011*, pp. 28-34, Apr. 2011.